

AD-A097 662

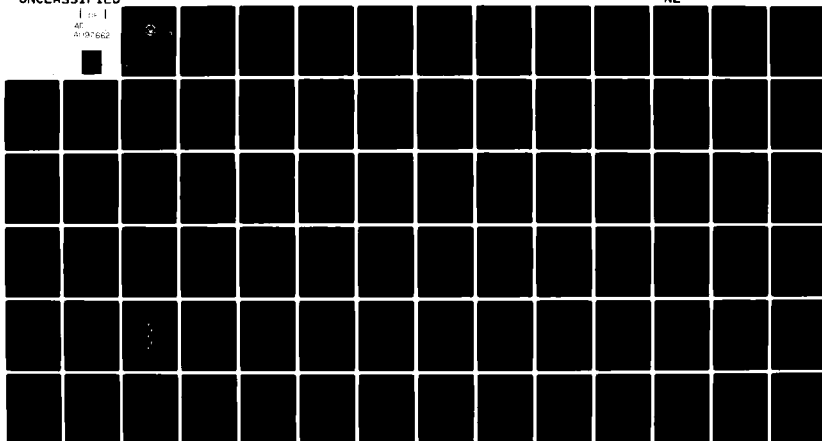
NAVAL POSTGRADUATE SCHOOL MONTEREY CA
THE EFFECT OF CONDENSATE INUNDATION ON CONDENSATION HEAT TRANSF--ETC(U)
DEC 80 I DEMIREL

F/G 13/1

UNCLASSIFIED

NL

1 1 1
AF
4/9/86Z



END
DATE
FILMED
5-81
DTIC

AD A 097 662

LEVEL

2

NAVAL POSTGRADUATE SCHOOL

Monterey, California



DTIC
SELECTED
APR 8 1981
C

THESIS

THE EFFECT OF CONDENSATE INUNDATION ON
CONDENSATION HEAT TRANSFER IN TUBE
BUNDLES OF MARINE CONDENSERS.

by

10

Ismail Demirel

11

Dec 1980

1283

Thesis Advisor:

P. J. Marto

Approved for public release; distribution unlimited

DTIC FILE COPY

81 4 13

002

REPORT DOCUMENTATION PAGE		READ INSTRUCTIONS BEFORE COMPLETING FORM
1. REPORT NUMBER	2. GOVT ACCESSION NO.	3. RECIPIENT'S CATALOG NUMBER
4. TITLE (and Subtitle) THE EFFECT OF CONDENSATE INUNDATION ON CONDENSATION HEAT TRANSFER IN TUBE BUNDLES OF MARINE CONDENSERS		5. TYPE OF REPORT & PERIOD COVERED Master's Thesis: December 1980
7. AUTHOR(s) Ismail Demirel		6. PERFORMING ORG. REPORT NUMBER
9. PERFORMING ORGANIZATION NAME AND ADDRESS Naval Postgraduate School Monterey, California 93940		8. CONTRACT OR GRANT NUMBER(s)
11. CONTROLLING OFFICE NAME AND ADDRESS Naval Postgraduate School Monterey, California 93940		10. PROGRAM ELEMENT, PROJECT, TASK AREA & WORK UNIT NUMBERS
14. MONITORING AGENCY NAME & ADDRESS (if different from Controlling Office) Naval Postgraduate School Monterey, California 93940		12. REPORT DATE December, 1980
		13. NUMBER OF PAGES 82
		15. SECURITY CLASS. (of this report) Unclassified
		16a. DECLASSIFICATION/DOWNGRADING SCHEDULE
16. DISTRIBUTION STATEMENT (of this Report) Approved for public release; distribution unlimited		
17. DISTRIBUTION STATEMENT (of the abstract entered in Block 20, if different from Report)		
18. SUPPLEMENTARY NOTES		
19. KEY WORDS (Continue on reverse side if necessary and identify by block number) Condensate inundation Heat Transfer Horizontal Tube Bundle Marine Condensers		
20. ABSTRACT (Continue on reverse side if necessary and identify by block number) Experiments, under different conditions, were conducted to evaluate the effect of condensate inundation on condensation heat transfer in tube bundles of marine condensers. Five 15.9 mm. (5/8 in) nominal outside diameter, smooth stainless steel tubes were used in a vertical row to simulate an actual condenser. Tubes were located in an equilateral triangular array with a spacing-to-diameter ratio of 1.5. Heat transfer performance was determined for each tube in a bundle. Data was taken for condensing steam on the outside of each tube at about		

DD FORM 1473
1 JAN 73EDITION OF 1 NOV 65 IS OBSOLETE
S/N 0102-014-6001

SECURITY CLASSIFICATION OF THIS PAGE (When Data Entered)

Block 20 (cont'd) 21 KPa (3 psia) and at about 101 KPa (14.7 psia). Each tube was cooled by water on the inside at velocities of 0.78 to 6.22 m/sec (2.56 ft/sec to 20.42 ft/sec). The overall heat transfer coefficient was determined directly from experimental data. The inside and outside heat transfer coefficients were determined using the Wilson plot technique.

Observation of condensate flow showed lateral droplet motion along the first three tubes in portions of the condenser under all conditions tested. Side drainage occurred only over the third and fourth tubes at a condensation pressure of about 21 KPa. The dominate mode of the flow at 101 KPa condensation pressure was gravitational flow. Outside heat transfer coefficients were higher than expected under all conditions when compared to the Nusselt theory. The reason for this is possibly due to secondary vapor flow. Recommendations to improve validations are provided. ←

Accession For	
NTIS GRA&I	<input checked="checked" type="checkbox"/>
DTIC TAB	<input type="checkbox"/>
Unannounced	<input type="checkbox"/>
Justification	
By	
Distribution/	
Availability Codes	
Dist	Avail and/or Special
A	

Approved for public release; distribution unlimited

The Effect of Condensate Inundation on
Condensation Heat Transfer in Tube
Bundles of Marine Condensers

by

Ismail Demirel
Lieutenant, Turkish Navy
B.S.M.E., Naval Postgraduate School, December 1979

Submitted in partial fulfillment of the
requirements for the degree of

MASTER OF SCIENCE IN MECHANICAL ENGINEERING

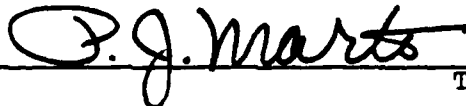
from the

NAVAL POSTGRADUATE SCHOOL
December, 1980

Author



Approved by:



Thesis Advisor



Chairman, Department of Mechanical Engineering



Dean of Science and Engineering

ABSTRACT

Experiments, under different conditions, were conducted to evaluate the effect of condensate inundation on condensation heat transfer in tube bundles of marine condensers. Five 15.9 mm. (5/8 in) nominal outside diameter, smooth stainless steel tubes were used in a vertical row to simulate an actual condenser. Tubes were located in an equilateral triangular array with a spacing-to-diameter ratio of 1.5.

Heat transfer performance was determined for each tube in a bundle. Data was taken for condensing steam on the outside of each tube at about 21 KPa (3 psia) and at about 101 KPa (14.7 psia). Each tube was cooled by water on the inside at velocities of 0.78 to 6.22 m/sec (2.56 ft/sec to 20.42 ft/sec). The overall heat transfer coefficient was determined directly from experimental data. The inside and outside heat transfer coefficients were determined using the Wilson plot technique.

Observation of condensate flow showed lateral droplet motion along the first three tubes in portions of the condenser under all conditions tested. Side drainage occurred only over the third and fourth tubes at a condensation pressure of about 21 KPa. The dominate mode of the flow at 101 KPa condensation pressure was gravitational flow. Outside heat transfer coefficients were higher than expected under all

conditions when compared to the Nusselt theory. The reason for this is possibly due to secondary vapor flow. Recommendations to improve validations are provided.

TABLE OF CONTENTS

I.	INTRODUCTION -----	13
	A. BACKGROUND INFORMATION -----	13
	B. OBJECTIVES OF THIS WORK -----	19
II.	EXPERIMENTAL APPARATUS -----	20
	A. INTRODUCTION -----	20
	B. STEAM SYSTEM -----	20
	C. TEST CONDENSER -----	21
	D. CONDENSATE SYSTEM -----	22
	E. COOLING WATER SYSTEM -----	23
	F. SECONDARY SYSTEMS -----	23
	1. VACUUM SYSTEM -----	23
	2. DESUPERHEATER -----	24
	G. INSTRUMENTATION -----	24
	1. FLOW RATES -----	24
	2. PRESSURE -----	25
	3. TEMPERATURE -----	25
	4. DATA COLLECTION AND DISPLAY -----	26
III.	EXPERIMENTAL PROCEDURES -----	27
	A. OPERATING PROCEDURES -----	27
	1. PREPARATION OF CONDENSER TUBES -----	27
	2. SYSTEM OPERATION AND STADY STATE CONDITIONS -----	27
	B. DATA REDUCTION PROCEDURES -----	28

1. OVERALL HEAT TRANSFER COEFFICIENT, U_n -----	28
2. CORRECTED OVERALL HEAT TRANSFER COEFFICIENT, U_c -----	29
3. INSIDE HEAT TRANSFER COEFFICIENT, h_i -----	30
4. OUTSIDE HEAT TRANSFER COEFFICIENT, h_o -----	30
C. DATA REDUCTION COMPUTER PROGRAM -----	31
IV. RESULTS AND DISCUSSION -----	32
V. CONCLUSIONS AND RECOMMENDATIONS -----	37
TABLES -----	38
FIGURES -----	56
APPENDIX A: TUBE CLEANING PROCEDURE -----	70
APPENDIX B: SAMPLE CALCULATIONS -----	71
APPENDIX C: ERROR ANALYSIS -----	75
LIST OF REFERENCES -----	80
INITIAL DISTRIBUTION LIST -----	82

LIST OF TABLES

I	LOCATION AND CHANNELS FOR THERMOCOUPLES -----	38
II	RUN CONDITIONS FOR RUNS 1-7 -----	39
III	RUN CONDITIONS FOR RUNS 8-12 -----	40
IV	RAW DATA FOR TUBE NO: 1, RUN 10 -----	41
V	RESULTS FOR TUBE NO: 1, RUN 10 -----	42
VI	RAW DATA FOR TUBE NO: 2, RUN 10 -----	43
VII	RESULTS FOR TUBE NO: 2, RUN 10 -----	44
VIII	RAW DATA FOR TUBE NO: 3, RUN 10 -----	45
IX	RESULTS FOR TUBE NO: 3, RUN 10 -----	46
X	RAW DATA FOR TUBE NO: 4, RUN 10 -----	47
XI	RESULTS FOR TUBE NO: 4, RUN 10 -----	48
XII	RAW DATA FOR TUBE NO: 5, RUN 10 -----	49
XIII	RESULTS FOR TUBE NO: 5, RUN 10 -----	50
XIV	CALCULATED U_n AND h_n FOR RUNS 10 AND 11 -----	51
XV	h_n VALUES FOR RUNS 1, 2 AND 3 -----	52
XVI	h_n VALUES FOR RUNS 4, 5 AND 6 -----	52
XVII	h_n VALUES FOR RUNS 7, 8 AND 9 -----	53
XVIII	h_n VALUES FOR RUNS 10, 11 AND 12 -----	53
XIX	\bar{h}_n/h_1 RATIO FOR RUNS 1, 2 AND 3 -----	54
XX	\bar{h}_n/h_1 RATIO FOR RUNS 4, 5 AND 6 -----	54
XXI	\bar{h}_n/h_1 RATIO FOR RUNS 7, 8 AND 9 -----	55
XXII	\bar{h}_n/h_1 RATIO FOR RUNS 10, 11 AND 12 -----	55

LIST OF FIGURES

1	DROPLET PATH THROUGH A TUBE BUNDLE WITH SIDE DRAINAGE -----	56
2	SCHEMATIC DIAGRAM OF STEAM SYSTEM -----	57
3	TEST CONDENSER SCHEMATIC, FRONT VIEW -----	58
4	SCHEMATIC SIDE VIEW OF TEST TUBE ARRANGEMENT -----	59
5	SCHEMATIC DIAGRAM OF CONDENSATE AND FEEDWATER SYSTEM -----	60
6	SCHEMATIC DIAGRAM OF COOLING WATER SYSTEM -----	61
7	SCHEMATIC DIAGRAM OF VACUUM SYSTEM -----	62
8	WILSON PLOT FOR TUBE NO: 1, RUN 10 -----	63
9	WILSON PLOT FOR TUBE NO: 2, RUN 10 -----	64
10	WILSON PLOT FOR TUBE NO: 3, RUN 10 -----	65
11	WILSON PLOT FOR TUBE NO: 4, RUN 10 -----	66
12	WILSON PLOT FOR TUBE NO: 5, RUN 10 -----	67
13	AVERAGE OUTSIDE HEAT TRANSFER COEFFICIENT RATIO VERSUS NO. OF TUBES FOR RUN 10 -----	68
14	AVERAGE OUTSIDE HEAT TRANSFER COEFFICIENT RATIO VERSUS NO. OF TUBES FOR RUN 7 -----	69

LIST OF SYMBOLS

A_n	OUTSIDE NOMINAL SURFACE AREA OF TUBE (m^2)
A_c	CROSS SECTIONAL AREA OF TEST SECTION (m^2)
C	CONSTANT DETERMINED FROM EXPERIMENTAL DATA
C_p	SPECIFIC HEAT (KJ/kg-°C)
C_{wv}	COOLING WATER VELOCITY (m/sec)
D_i	TUBE INSIDE DIAMETER (m)
D_o	TUBE OUTSIDE DIAMETER (m)
G	MASS FLOW RATE OF COOLING WATER PER UNIT AREA (kg/m^2 -sec)
GPM	GALLONS PER MINUTE OF COOLING WATER FLOW
h_{fg}	LATENT HEAT OF VAPORIZATION (J/kg)
h_i	INSIDE HEAT TRANSFER COEFFICIENT (W/m^2 -°C)
h_o	OUTSIDE HEAT TRANSFER COEFFICIENT (W/m^2 -°C)
h_n	MEAN HEAT TRANSFER COEFFICIENT ON n^{th} TUBE (W/m^2 -°C)
\bar{h}_n	AVERAGE HEAT TRANSFER COEFFICIENT OVER A BUNDLE OF n TUBES (W/m^2 -°C)
h_{Nu}	NUSSELT'S HEAT TRANSFER COEFFICIENT (W/m -°C)
k_w	THERMAL CONDUCTIVITY OF WATER (W/m -°C)
L	LENGTH (m)
LPM	LITERS PER MINUTE
M	SLOPE OF WILSON PLOT

\dot{m}_c	MASS FLOW RATE OF CONDENSATE (kg/sec)
\dot{m}_{cw}	MASS FLOW RATE OF COOLING WATER (kg/sec)
n	NUMBER OF TUBES
μ	DYNAMIC VISCOSITY (kg/m-sec)
Pr	PRANDTL NUMBER
Q	HEAT TRANSFER RATE (J/sec)
Re	REYNOLDS NUMBER
ρ	DENSITY (kg/m ³)
R_w	WALL RESISTANCE (m ² -°C/W)
T_{bc}	BULK TEMPERATURE (°C)
T_{bk}	BULK TEMPERATURE (K)
T_{ci}	COOLING WATER INLET TEMPERATURE (°C)
T_{co}	COOLING WATER OUTLET TEMPERATURE (°C)
T_{hw}	CONDENSATE TEMPERATURE IN PRIMARY HOTWELL (°C)
T_{shw}	CONDENSATE TEMPERATURE IN SECONDARY HOTWELL (°C)
T_v	SATURATION TEMPERATURE OF VAPOR (°C)
\bar{T}_w	AVERAGE WALL TEMPERATURE OF THE TUBE (°C)
U_c	CORRECTED OVERALL HEAT TRANSFER COEFFICIENT (W/m ² -°C)
U_n	OVERALL HEAT TRANSFER COEFFICIENT (W/m ² -°C)
X	ABSCISSA OF WILSON PLOT
Y	ORDINATE OF WILSON PLOT (m ² -°C/W)

ACKNOWLEDGEMENT

The author wishes to express his sincerest appreciation of the many helpful suggestions and kind advice given him during course of this work by Professor Paul J. Marto of the Department of the Mechanical Engineering. A special note of thanks is deserved by Mr. Ken Mothersell for his technical and skillful support during this project.

I would also like to thank my wife Mevlude["], for her understanding, sacrifice and moral support.

I. INTRODUCTION

A. BACKGROUND INFORMATION

Recent improvements in turbine machinery and boiler design have brought about an increase in horsepower to weight ratio of marine propulsion systems. However there has been no similar improvement, in practice, in the steam plant condenser size.

Practical marine steam condenser design is based almost exclusively upon two documents. The Heat Exchange Institute (HEI) standards for steam surface condensers [1] and the standards of Tubular Exchange Manufacturers Association (TEMA) [2]. These standards have proven to be reliable. But it is evident that the resulting condensers are significantly oversized. Briefly, Search [3] has shown that heat transfer enhancement methods could decrease condenser space to weight ratio, thereby establishing new design criteria for marine condensers.

It has been the objective of past research by Eshleman [4] to investigate the effect of condensate inundation on heat transfer in a horizontal tube bundle. But, his research concentrated on designing, constructing and validating the test facility.

Since the publication of Nusselt's well-known theoretical paper [5] on film condensation many theoretical and experimental studies have occurred.

The evaluation of the heat transfer coefficient from the vapor condensing on the outer surface of horizontal tubes is based mainly on Nusselt's theoretical formulas.

Nusselt performed the derivation and found that the average heat transfer coefficient \bar{h}_n for n tubes located below one another is,

$$\bar{h}_n = 0.725 \left[\frac{\rho_f (\rho_f - \rho_v) h_{fg} k_f^3 g}{n \mu_f D_o (T_{sv} - \bar{T}_w)} \right]^{1/4} \quad (1)$$

where k_f : Thermal conductivity of film (W/m- C)

\bar{T}_w : Average tube wall temperature (C)

ρ_f : Film density (kg/m³)

ρ_v : Vapor density (kg/m³)

μ_f : Dynamic viscosity of film (kg/m-sec)

g : Acceleration of gravity (m/sec²)

For the uppermost tube, equation (1) becomes

$$h_{Nu} = 0.725 \left[\frac{\rho_f (\rho_f - \rho_v) h_{fg} k_f^3 g}{\mu_f D_o (T_{sv} - \bar{T}_w)} \right]^{1/4} \quad (2)$$

Hence, the relationship between the average heat transfer coefficient for a horizontal tube bundle (\bar{h}_n) consisting of n tubes and the mean heat transfer coefficient (h_{Nu}) for the uppermost tube may be found as,

$$\bar{h}_n / h_{Nu} = n^{-1/4} \quad (3)$$

The above equations were derived by Nusselt assuming:

1. Condensation of a saturated vapor at negligible velocity,

2. Laminar flow of the condensate film in a continuous sheet from one tube to the next at a constant temperature difference for all tubes in the bank.

In actual condensers, vapor moves at a fairly high speed over a considerable part of its path. Under changing turbine speeds, steam velocity is not negligible. But attempts to evaluate analytically the effect of vapor velocity have not been successful. The vapor velocity causes friction between the vapor and the condensate film. With downward flow of vapor and condensate (as in our experiment) the frictional forces are added to the force of gravity. Consequently as the film velocity increases, the thickness of the film decreases and the coefficient of heat transfer from vapor to wall increases.

Additionally, the condensate does not flow down from each tube in a continuous film. Rather it forms drops or streams. Condensate dripping on a tube from above splits around the tube but does not flow axially. The thickness of the film caused by the condensate coming down from above is thus confined to the place where the drops and streams descend, which causes local disturbances in film flow. Briefly, the true nature of condensate flow on and between tubes differs from the flows assumed by Nusselt.

Recently, Eissenberg [6] noted that the condensate droplets formed on the tubes strike anywhere on the lower half of the tubes below. His experimental results gave heat transfer coefficients well above those predicted by Nusselt.

Eissenberg proposed a side drainage model, and formulated that,

$$\bar{h}_n / h_{Nu} = 0.6 + 0.42 n^{-1/4} \quad (4)$$

As a matter of fact, it can be said that in most cases experimental data has been fit to various modified forms of equation (5) below:

$$\bar{h}_n / h_{Nu} = n^{-s} \quad (5)$$

where $0.07 \leq s \leq 0.223$.

Generally, the effects of condensate inundation and vapor velocity are described separately from each other. Actually, they occur simultaneously and their combined effect is complex. Fujii [7] correlated the effect of inundation and vapor shear by using experimental data of Nobbs and Mayhew [8, 9]. The data for in-line tube banks resulted in equations (6) and (7).

$$Nu_m^o = 10.74 Re_L^{0.312} \quad (6)$$

Equation (6) above is an experimental equation for a tube without inundation where

Nu_m^o : Nusselt number, $(h_o d_o / k_L)$ for pure steam, also without inundation.

Re_L : Two phase Reynolds number, $(U_\infty d_o / \nu_L)$

k_L : Thermal conductivity of liquid

d_o : Tube outside diameter

ν_L : Kinematic viscosity of liquid

and U_∞ : Vapor velocity

Nu_m/Nu_m^O is computed for the data with inundated tubes and equation (7) is derived.

$$Nu_m/Nu_m^O = (Re_L/2 \times 10^6)^{0.071} (w/w^O)^{0.65} \quad (7)$$

Nu_m : Mean Nusselt number for a tube

w : Rate of inundation falling onto a tube

w^O : Rate of condensation of a tube corresponding to Nu_m^O .

For the staggered tube bank, a correlation was not obtained by Fujii. Fujii determined that for the staggered tube bank, the inundation effect was smaller than that for the in-line bank. This would follow from examination of Eissenberg's side drainage model.

Chisholm [10] combined the developments of Berman and Tumanov [11], and Fuks [12] into one equation to evaluate the effects of condensate inundation, vapor velocity and non-condensable gas in tube bundles. Chisholm has given the following formula for heat flux,

$$q = C_h (T_s - T_w)^{3/4} \quad (8)$$

where

$$C_h = 0.725 \left[\frac{K_c^3 L g}{D_o \mu_c V_c^2} \right]^{1/4} \left\{ 1 + \frac{\sum_{r=1}^{n-1} w_{c,r}}{w_{c,n-1}} \right\}^{-0.07} (1 + 0.0095 Re_m^{11.8} / \sqrt{Nu}) \quad (9)$$

Equation (9) is for the downward flow of the vapor.

T_s : Temperature of condensate surface ($^{\circ}\text{C}$)

T_w : Temperature of outer tube wall ($^{\circ}\text{C}$)

K_c : Thermal conductivity of condensate ($\text{W/m-}^{\circ}\text{C}$)

L : Specific latent heat (J/kg)

μ_c : Absolute viscosity of condensate (kg/m-sec)

v_c : Specific volume of condensate (m^3/kg)

$w_{c,r}$: Rate of condensation of rth tube row (kg/sec)

Re_m : Reynolds number of vapor-gas mixture.

In the above equation,

$$Nu = \frac{\alpha_{stat}^D o}{K_c} \quad (10)$$

where α_{stat} : Heat transfer coefficient across the condensate film, static vapor condition ($\text{W/m}^2\text{-C}$)

Experimental data resulting from varying inundation rates and vapor velocities is sufficiently scattered to suggest that no existing correlation fits all the available data (some of the available data is related to enhanced tubes). This is because there are so many variables that affect marine condenser performance, some of which have to be discovered (e.g., non-condensable gas effects, pitch-to-diameter ratio of condenser tubes, direction of vapor flow, and the effects due to ship motion in three dimension). Research is presently being conducted in the United Kingdom aimed at producing a model of condensation suitable for sophisticated condenser performance calculations. However, the results have yet to be published.

B. OBJECTIVES OF THIS WORK

In order to evaluate the effect of inundation on a bank of enhanced tubes, it was necessary to establish data on a bank of smooth tubes as a standard of comparison. The objectives of this work were therefore: (1) to establish experimental data on a bank of smooth tubes as a standard, and (2) to compare the established data to theoretical predictions.

II. EXPERIMENTAL APPARATUS

A. INTRODUCTION

The existing test facility was designed by Beck [11] and built and tested by Pence [12]. Major modifications were made to the original apparatus by Eshleman [4]. During this work, some minor modifications were made and these changes are given in Tables II and III for each run.

B. STEAM SYSTEM

The steam system is shown in Figure 2. The supply of steam is locally generated and supplied to the building which houses the experimental apparatus. The steam is provided by means of a 19.05 mm. diameter line and a steam inlet valve (MS-2). A compound pressure gage is located just prior to the steam separator which monitors the supply pressure as it is adjusted by (MS-2). Following the steam separator, a line strainer provides additional protection from contamination. After the strainer, the steam proceeds through a 31.75 mm. diameter line which provides for two possible steam paths. The primary path for system operation is via the throttling valve (MS-3), through a desuperheater and into the test condenser. Inside the condenser, the steam is condensed on the test tubes. The steam which is not condensed proceeds via the vapor outlet on the test condenser to the secondary condenser. The secondary

steam flow path is used to accomplish system stabilization during startup and to control the mass flow rate of steam to the condenser during operation. Steam proceeds via (MS-4) directly to the secondary condenser. All steam lines except the primary path downstream of (MS-3) were insulated with 25.4 mm. thick fiberglass insulation.

C. TEST CONDENSER

The test condenser is shown from various views in Figures 3 and 4. Steam enters via the top and proceeds over the baffle separators and through a flow straightener, which is covered with three layers of 150 mesh screen, to the tube bundle. The condensate collects at the bottom of the condenser and flows out one of the two 12.7 mm. diameter openings at either end of the condenser to the hotwell where it can be collected and measured.

Three separate viewing windows each 203 mm. by 140 mm. by 17.7 mm. and made of pyrex plate glass had been installed to provide maximum viewing of the active tubes.

The tube sheet arrangement is shown in Figure 4. The tubes were arranged in a typical naval condenser spacing-to-diameter ratio of 1.5. They were 15.9 mm. OD, 1.14 mm. thick, 304 stainless steel tubes that had cooling water passing through them. Although typical naval condenser tubes are made of 90-10 copper-nickel, the choice of 304 stainless steel was based on "on hand" stock and the fact that the principles of inundation

do not depend on the tube material although perhaps the heat flux may change due to different wall resistance. The remaining half tubes were made of 15.9 mm. OD aluminum bar stock and were fastened by screws to the outside wall of the steam flow path. This arrangement was selected to best simulate the steam flow conditions in a section of an actual condenser. The five test tubes are singularly removable. The top tube can be replaced by a 304 stainless steel porous tube which could simulate various condensate inundation rates.

The test condenser was insulated with a 25.4 mm. thick sheet of Armorflex insulation.

D. CONDENSATE SYSTEM

The condensate system is shown in Figure 5. The condenser hotwell collects the condensate from the test tubes, while the secondary condenser hotwell collects the condensate from the secondary condenser. Valve (C-1) allows the isolation of the test condenser hotwell for condensate measurement. Since house steam was used as the steam supply system, the condensate collected in the hotwells is pumped back to the house system by the condensate pump via valve (C-3). The condensate lines were insulated with 19.1 mm. thick Johns-Manville Aerotube insulation.

E. COOLING WATER SYSTEM

The cooling water system is shown in Figure 6. The water used was normal house water which had been passed through a water softener on the way to the supply tank. The water is pumped from the supply tank by a 5 HP electric driven pump. It is routed to the flowmeter header via 51 mm. OD plastic pipe. The flow of cooling water for each test tube is then individually controlled and measured by it's own rotometer. Each rotometer allowed a maximum flow rate of 70.4 LPM. The heated cooling water, after passing through the test section, was piped back to a supply tank. A separate system pumped this heated water through a filter and cooling tower returning the cooled water to the supply tank in an effort to maintain a constant cooling water inlet temperature.

After leaving the rotometers, the system piping was reduced to 15.9 mm., ensuring a distance of 1 m. ahead of the test section to ensure a hydrodynamically fully developed velocity profile while passing through the test section.

F. SECONDARY SYSTEMS

1. Vacuum System

The vacuum in the test condenser and secondary condenser was maintained by a mechanical vacuum pump and a vacuum regulator which induces air into the system. The vacuum pump takes a suction from the secondary condenser hotwell which is connected to the test condenser hotwell via discharge piping. A cold

trap at the inlet of the vacuum pump forces incoming vapor to pass over a system of refrigerated copper coils. This removes steam and entrained water from the vacuum line preventing moisture contamination of the vacuum pump oil. The vacuum pump outlet is vented through a roof exhaust fan to avoid a health hazard from breathing any oil vapor exhausted by the pump. A schematic diagram of this system can be found in Figure 7.

2. Desuperheater System

The desuperheater removes sensible heat from the superheated steam by injecting water at about 25°C via the existing feedwater system through valve (DS-1) and a rotometer. The desuperheater is a 267 mm. diameter stainless steel can, 457 mm. high, having four nozzles inserted equidistant around the circumference of the inner top of the can. The nozzles are a fan type and are positioned such that the spray is downward at a 45° angle to allow for better mixing. A collection tank is located on the bottom of the desuperheater to allow for drainage of condensate. This system can be isolated by valve (DS-2)

G. INSTRUMENTATION

1. Flow rate

a. Steam velocity was determined by calculation

$$U_s = \frac{\dot{m}_c v}{A_c} \quad (11)$$

where

$$\begin{aligned}\dot{m}_c &= \text{Mass flow rate of condensate (kg/sec)} \\ &= Q/h_{fg}\end{aligned}$$

$$A_c = \text{Cross sectional flow area (m}^2\text{)}$$

$$\text{and } v = \text{Specific volume of vapor (m}^3\text{/kg)}$$

b. Cooling water flow rate was measured individually for the five separate tubes. Each flow rate was determined by a rotometer with a capacity of 70.4 LPM (18.6 GPM). The calibration procedure used was identical to that listed in Appendix A of Ref. [14].

2. Pressure

Two different pressure sensing devices were used during experimentation. They were a Bourdon tube pressure gauge which measured steam pressure and an absolute pressure transducer coupled with a 760 mm. mercury manometer which was used to measure test condenser pressure.

3. Temperature

Stainless steel sheathed , copper-constantan thermocouples were used as the primary temperature monitoring devices. Figure 3 shows the location of five vapor thermocouples. The remaining 30 thermocouples of this type were located as shown in Figure 6, six on each tube, two measuring cooling water inlet temperature and four measuring water outlet temperature. Calibration procedures of the thermocouples were identical to those listed in Appendix A of Ref. [16].

4. Data Collection and Display

An Autodata collection system was utilized to record and display the temperatures in degrees celsius obtained from the primary stainless steel thermocouples. Table I lists the channel numbers and location of these devices.

III. EXPERIMENTAL PROCEDURES

A. OPERATING PROCEDURES

1. Preparation of condenser tubes

Prior to any run, each tube was properly prepared to ensure filmwise condensation. The cleaning procedure for stainless steel tubes is listed in Appendix A.

2. System operation and steady state conditions

The basic operating instructions developed by Pence [14] and modified by Reilly [15] were used. The only difference in the procedure as listed in Appendix B of Ref. 16 was that instead of one cooling water flowmeter to adjust, the experimenter had five to set as desired.

In general it took about three hours from initial light-off until steady-state conditions were established. The parameters used in determining steady-state conditions were cooling water inlet temperature and steam inlet temperature. If the cooling water inlet did not vary more than ± 0.6 °C/hr and the steam temperature did not vary more than ± 0.3 °C/min, steady-state was considered achieved.

The time for the system to stabilize between changes in cooling water flow rate during the Wilson plot technique was approximately twenty minutes. This time increment is suspect as other investigators waited about one hour for stabilization between changes, especially for atmospheric runs.

It must be pointed out however that the amount of time required to collect data over five tubes in a system that can't be shut down and repeated the next day prohibits the greater time increment between data points for the Wilson plot.

The general set up for the data taken in this research was a steam velocity of between approximately 1.2 m/sec and 1.4 m/sec, steam temperature of 62 °C or 75 °C for 21kPa condensation conditions and 100 °C for atmospheric (101 kPa) runs.

B. DATA REDUCTION PROCEDURE

The raw data collected for each tube for run 10 can be found in the Tables beginning on page 38.

Appendix B, the sample calculations, is a complete listing of the equations used to evaluate the data. Appendix C is a derivation of the probable error in the data reduction equations, followed by a sample error analysis for tube number 1 at 40 percent flow, run 10.

The following standard heat transfer equations were used to reduce the raw data into a form that can be used for evaluation.

1. Overall heat transfer coefficient (U_o)

The method employed to arrive at the overall heat transfer coefficient is straightforward and similar to that employed by many researchers in the past. The heat transfer rate to the cooling water is given by

$$Q = \dot{m} C_p (T_{co} - T_{ci}) \quad (12)$$

The heat transfer rate from the steam is given by,

$$Q = \dot{m}_{con} [C_{pv}(T_v - T_{sat}) + h_{fg} + C_{p(con)}(T_{sat} - T_{con})] \quad (13)$$

The heat transfer rate can also be found from the overall heat transfer coefficient by

$$Q = U_n A_n (LMTD) \quad (14)$$

where

$$LMTD = \frac{(T_v - T_{ci}) - (T_v - T_{co})}{\ln (T_v - T_{ci}) / (T_v - T_{co})} \quad (15)$$

After combining equations (12), (14), and (15) it can be found that

$$U_n = \frac{\dot{m} C_p}{A_n} \ln \frac{T_v - T_{ci}}{T_v - T_{co}} \quad (16)$$

2. Corrected overall heat transfer coefficient (U_c)

$$U_c = \frac{1}{\frac{1}{U_n} - R_w} \quad (17)$$

where R_w is the wall resistance corresponding to different tube materials and may be given by

$$R_w = \frac{A_n \ln(r_o/r_i)}{2 \pi k_w L_{ts}} \quad (18)$$

where L_{ts} is the length of the tube.

Equation (17) allows for the comparison of tubes of different materials for the same steam and cooling water condition within the test condenser.

3. Inside heat transfer coefficient (h_i)

$$Nu = \frac{h_i D_i}{k} = 0.036 Re^{0.8} Pr^{1/3} (L/D)^{-0.054} \quad (19)$$

Equation (19) was selected because both the Dittus-Boelter and Sieder-Tate relationships which are commonly used assume a fully developed velocity, as well as a fully developed thermal profile. In this research, it was suspected that, although the velocity profile was believed to be fully developed, the thermal profile was not fully developed. When an L/D ratio of 57.6 is used in equation (19) a constant of 0.029 results. This was validated by computing the average of all the tube constants obtained as a result of the Wilson plot technique. Wilson plots for each tube for run 10 can be found in Figures 8 through 12.

4. Outside heat transfer coefficient (h_o)

The outside heat transfer coefficient is the parameter that is used to compare results of each tube in the bundle and is given by

$$h_o = \frac{1}{(1/U_n) - R_w - (D_o/D_i h_i)} \quad (20)$$

Two very important assumptions were made in using this equation.

a. The resistance due to fouling was equal to zero. This assumption is supported by the fact that the tubes were new, chemically cleaned and smooth. Also, treated soft water was used as the cooling medium.

b. The resistance due to non-condensable gases was equal to zero. This assumption was supported by the fact that the system was tested for air-tightness and found to be secure. In addition, it was believed that the velocity of steam passing through the test section was sufficiently large to keep the system purged of any non-condensables that might collect in the test section.

C. DATA REDUCTION COMPUTER PROGRAM

Reilly [15] developed the existing program in Fortran Language. His program had been translated into Basic Language for use with the HP 9845 computer by Eshleman [4] during his work. Ultimately, this program with minor modifications, can be used in an integrated system between the Autodata Nine data collector and the HP 9845 computer. This will allow automatic data input with real time data output for the experimenter. During this work, the existing computer program of Eshleman [4] for reduction of data was used with the HP 9845 computer.

IV. RESULTS AND DISCUSSION

The experiments were done by using two different condensation pressures to establish experimental data on a bank of smooth tubes. Condensation pressure for runs 1 through 5 and 9 through 12 was maintained at about 3 psia. For runs 6, 7, and 8 the pressure was maintained at atmospheric conditions. Runs 8, 9, and 2 were repetitions of runs 7, 5, and 1 respectively. Experimental conditions are given in Tables II and III for each run.

In equation (16), the T_v term stands for vapor temperature. Large differences in the heat transfer coefficients were obtained depending on whether the actual vapor temperature or the saturation temperature was used in equation (16). It is worthwhile to note that the outside heat transfer coefficients using the actual, superheated steam temperatures were 52 percent lower than those calculated using the saturation temperature. The percent change of U_n values was 79 percent. To overcome this interesting result, it was decided that the T_v term in equation (16) must be the saturation temperature instead of actual vapor temperature. For comparison U_n and h_n values are tabulated in Table XIV for runs 10 (saturated) and 11 (superheat) in which T_v was actual vapor temperature. Saturation temperature was therefore used in equation (16) for all runs except those reported in Table XIV.

The runs, conducted at 3 psia condensation pressure, gave unexpected results. Outside heat transfer coefficients for the five test tubes showed significant fluctuations. The values of \bar{h}_n decreased for the first three tubes and then increased. Generally, for all runs conducted at 3 psia, the heat transfer coefficients followed this same pattern. The cause for this behavior may be due to several phenomena.

During observation of the condensate flow pattern on the first three tubes, there was evidence of lateral droplet migration. This migration was due presumably to a deflection of these tubes or due to axial flow of vapor. This causes a non-uniform heat transfer rate across the length of the tube because of a decrease in film thickness at some locations and then an increase in film thickness in other locations. This thickening of the film on the tubes would result in a lower average heat transfer coefficient than expected. Secondly, steam appeared to concentrate at the bottom of the test condenser, and may have caused cross flow around the lower tubes. This may have been caused by a system resistance to the flow of excess steam which is not condensed in the test condenser. Circulating flow of the excess steam which could not easily leave the test condenser may have caused side drainage of the condensate. It was observed that the condensate flow path on the fourth and fifth tubes was toward the observation window. Because of these two reasons, the outside heat transfer coefficients for the last

two tubes would be high. As an example, Table XXII lists values for run 10, and these are plotted in Figure 13 along with two theoretical results.

Figures 8 through 12 are the Wilson plots that assist in determining the constant in equation (19). As an example, run 10 was chosen and the results are plotted in these Figures. All tubes yield good linear plots with slopes which provide constants of 0.028, 0.032, 0.032, 0.028 and 0.030 respectively. The expected linear plots were obtained for all the other runs as well as run 10. The data reduction program gives the option of using the constant solved for via the Wilson plot technique or inputting one of the user's own choosing. In this work, for all runs, 0.029 was used as input for all the tubes to determine the inside heat transfer coefficient which in turn was then used in the determination of the outside heat transfer coefficient. Outside heat transfer coefficients for all runs are tabulated in Tables XV through XVIII.

The ratio of \bar{h}_n/h_1 as listed in Tables XIX through XXII for all runs, was determined by taking the average outside heat transfer coefficient h_o for n tubes and averaging them, then dividing by the outside heat transfer coefficient of the first tube (h_1). The results of run 7, as listed in Table XXI, are plotted on Figure 14 along with the theoretical equations of Nusselt and Eissenberg. Based on the observations of condensate flow at atmospheric pressure, the data

for all tubes was expected to fall closer to the Nusselt curve due to the presence of gravity dominated flow, but certainly not below it.

The experimental study on the effect of the vapor velocity upon condensation was performed both at 3 psia and 14.7 psia condensation pressure. Runs 9 and 10 at 3 psia, and runs 6 and 7 at atmospheric pressure were conducted at different vapor velocity to determine the effect of vapor velocity. Vapor velocities for runs 10 and 7 were slightly higher than runs 9 and 6 respectively. The experimental result for the 3 psia pressure case was unexpected. This result may be due to the effect of saturated steam. At atmospheric pressure, for the higher vapor velocity, the heat transfer coefficient was higher as expected.

From examination of the results of runs 7, 8 and 10, 11 it may be said that at higher condensation pressure, the heat transfer coefficient is higher.

Each repeated run was within the uncertainty range of the original. The conclusion is that the data obtained for ten runs is sufficient to make comparison between results.

Side pieces and baffles were installed inside the test condenser to prevent axial flow of the vapor. However droplet migration still resulted in both cases. From the comparison of the run 11 and 12, it may be concluded that side pieces generally did not have any effect on the heat transfer coefficient. Heat transfer coefficients of runs 11 and 12

are within the uncertainty range of each other. The difference between heat transfer coefficients of runs 4 and 10 is due to effect of baffles. Outside heat transfer coefficients are higher at run 4 because of the baffles that form a path for the condensate.

V. CONCLUSIONS AND RECOMMENDATIONS

The experimental data obtained lead to the following conclusions:

1. There is evidence of secondary flow of steam within the test condenser which is suspected to have influenced the results.
2. Equation (16) should not be used with superheated steam temperatures.
3. The measured ratio of \bar{h}_n/h_1 is lower than expected at atmospheric runs.

The following recommendations are provided:

1. Improve the steam flow path to ensure a uniform downward profile through the tube bundle. This can be accomplished by re-design of the steam inlet section.
2. Prevent auxiliary system resistance against the flow of uncondensed steam when working at vacuum. This can be done by either conducting experiments at atmospheric pressure or by re-designing the auxiliary system piping with large diameter.
3. Instrument the top tube with thermocouples to measure \bar{T}_w in order to check the outside heat transfer coefficient against the Nusselt theory.
4. Measure the vapor pressure between tubes to get more accurate calculations.

TABLES

TABLE I

LOCATION OF STAINLESS STEEL SHEATHED COPPER-CONSTANTAN THERMOCOUPLES

<u>CHANNEL NUMBER</u>	<u>LOCATION</u>	<u>CHANNEL NUMBER</u>	<u>LOCATION</u>
52	T_{hw}	82	T_{∞} # 2
64	T_{shw}	83	T_{∞} # 2
65	T_v	84	T_{∞} # 2
66	T_v	85	T_{∞} # 2
67	T_v	86	T_{∞} # 3
68	T_v	87	T_{∞} # 3
69	T_v	88	T_{∞} # 3
70	T_{ci} # 1	89	T_{∞} # 3
71	T_{ci} # 1	90	T_{ci} # 5
72	T_{ci} # 2	91	T_{ci} # 5
73	T_{ci} # 2	92	T_{∞} # 4
74	T_{ci} # 3	93	T_{∞} # 4
75	T_{ci} # 3	94	T_{∞} # 4
76	T_{∞} # 1	95	T_{∞} # 4
77	T_{∞} # 1	96	T_{∞} # 5
78	T_{∞} # 1	97	T_{∞} # 5
79	T_{∞} # 1	98	T_{∞} # 5
80	T_{ci} # 4	99	T_{∞} # 5
81	T_{ci} # 4		

TABLE II
RUN CONDITIONS FOR RUN 1 THROUGH 7

Run No.	CONDITIONS
1	Condensation pressure 3 psia., Superheat steam, Low vapor velocity.
2	Same as Run No: 1
3	Condensation pressure 3 psia., Superheat steam, Low vapor velocity, Steam gage has been changed.
4	Condensation pressure 3 psia., Saturated steam, Low vapor velocity, Baffles and Vacuum control valve have been installed, Throttle valve has been changed.
5	Same as Run No: 4
6	Condensation pressure atmospheric, Saturated steam, Low vapor velocity, Baffles have been removed.
7	Condensation pressure atmospheric, Saturated steam, High vapor velocity.

TABLE III
RUN CONDITIONS FOR RUN 8 THROUGH 12

Run No.	CONDITIONS
8	Same as Run No. 7
9	Condensation pressure 3 psia, Saturated steam, Low vapor velocity.
10	Condensation pressure 3 psia., Saturated steam, High vapor velocity.
11	Condensation pressure 3 psia., Superheat steam, High vapor velocity.
12	Condensation pressure 3 psia., Superheat steam, High vapor velocity, Side pieces have been installed.

TABLE IV

RAW DATA FOR TUBE NO: 1, RUN 10

<u>3 FLOW</u>	<u>T_{ci} (°C)</u>	<u>T_{co} (°C)</u>	<u>T_v (°C)</u>	<u>GPM</u>
10	24.950	36.067	73.375	1.92
12.5	25.250	34.325	73.375	2.40
15	25.750	34.767	73.375	2.88
17.5	26.550	34.767	73.375	3.36
20	27.100	34.467	73.375	3.84
25	26.450	32.200	73.375	4.80
40	27.700	32.700	73.375	7.68
50	28.700	33.167	73.375	9.67
70	30.100	33.533	73.375	13.48
80	31.050	34.133	73.375	15.36

TABLE V

RESULTS FOR TUBE NO: 1, RUN 10

$\underline{U_n}$	$\underline{U_c}$	\underline{Q}	$\underline{\dot{m}_c}$
2906.755	3486.533	5649.880	.002405
2912.181	3494.363	5767.253	.002455
3509.480	4391.116	6874.909	.002926
3763.169	4795.622	7307.513	.003111
3864.645	4961.648	7487.057	.003187
3644.438	4604.459	7310.103	.003112
5169.389	7340.180	10166.006	.004327
5912.132	8933.959	11431.371	.004866
6463.177	10255.078	12241.189	.005211
6736.134	10959.733	12521.407	.005330

$\underline{h_i}$	$\underline{h_o}$	\underline{C}	\underline{Re}	$\underline{C_{wv}}$
4598.834	23811.652	0.029	14054.5	.78
5453.646	12542.547	0.029	17314.4	.97
6343.280	19904.566	0.029	20975.3	1.17
7207.769	19113.540	0.029	24669.7	1.36
8031.485	16296.772	0.029	28264.7	1.55
9446.257	10204.903	0.029	34305.3	1.94
13893.319	18116.447	0.029	55869.9	3.11
16841.966	22180.994	0.029	71391.4	3.91
22183.212	21386.404	0.029	101287.7	5.46
24834.745	21782.715	0.029	117197.2	6.22

TABLE VI

RAW DATA FOR TUBE NO: 2, RUN 10

<u>% FLOW</u>	<u>T_{ci} (°C)</u>	<u>T_{co} (°C)</u>	<u>T_v (°C)</u>	<u>GPM</u>
10	25.000	35.425	73.375	1.92
12.5	25.300	34.325	73.375	2.40
15	25.850	34.150	73.375	2.88
17.5	26.600	34.175	73.375	3.36
20	27.100	33.825	73.375	3.84
25	26.250	32.450	73.375	4.80
40	27.750	32.025	73.375	7.68
50	28.800	32.500	73.375	9.67
70	30.200	32.850	73.375	13.48
80	31.100	33.500	73.375	15.36

TABLE VII

RESULTS FOR TUBE NO: 2, RUN 10

$\underline{U_n}$	$\underline{U_c}$	\underline{Q}	$\underline{\dot{m}_c}$
2705.496	3200.943	5298.997	.002256
2897.657	3473.472	5735.404	.002441
3209.670	3931.614	6328.988	.002694
3446.036	4292.242	6737.508	.002868
3500.473	4377.025	6835.719	.002910
3932.755	5074.475	7882.096	.003355
4387.397	5857.697	8693.329	.003700
4863.757	6738.890	9469.938	.004031
4953.877	6913.138	9450.620	.004023
5206.388	7415.001	9748.893	.004150

$\underline{h_i}$	$\underline{h_o}$	\underline{C}	\underline{Re}	$\underline{C_{wv}}$
4583.724	14974.334	0.029	13971.0	.78
5455.170	12268.806	0.029	17323.2	.97
6325.033	13098.673	0.029	20866.8	1.17
7186.119	13105.593	0.029	24535.6	1.36
8002.946	11391.899	0.029	28083.1	1.55
9448.909	12835.402	0.029	34322.7	1.94
13844.978	11186.354	0.029	55518.4	3.11
16789.189	12295.258	0.029	70986.6	3.91
22112.360	10668.317	0.029	100702.3	5.46
24756.032	11187.876	0.029	116524.8	6.22

TABLE VIII

RAW DATA FOR TUBE NO: 3, RUN 10

<u>% FLOW</u>	<u>T_{ci} (°C)</u>	<u>T_{co} (°C)</u>	<u>T_v (°C)</u>	<u>GPM</u>
10	25.025	35.450	73.375	1.92
12.5	25.300	34.325	73.375	2.40
15	25.800	34.125	73.375	2.88
17.5	26.600	34.100	73.375	3.36
20	27.100	33.725	73.375	3.84
25	26.500	32.400	73.375	4.80
40	27.750	32.000	73.375	7.68
50	28.800	32.500	73.375	9.67
70	30.200	32.775	73.375	13.48
80	31.100	33.425	73.375	15.36

TABLE IX

RESULTS FOR TUBE NO: 3, RUN 10

U_n	U_c	Q	\dot{m}_c
2701.263	3195.018	5286.187	.002250
2897.657	3473.472	5735.404	.002441
3216.662	3942.109	6348.174	.002702
3408.819	4234.655	6670.928	.002840
3444.271	4289.504	6734.245	.002866
3750.225	4774.622	7500.319	.003193
4360.472	5809.799	8642.547	.003679
4863.757	6738.890	9469.938	.004031
4809.363	6634.918	9183.326	.003909
5039.093	7080.227	9444.421	.004020

h_i	h_o	C	Re	C_{wv}
4585.638	14822.994	0.029	13981.6	.78
5455.170	12268.806	0.029	17323.2	.97
6322.386	13228.923	0.029	20851.0	1.17
7183.124	12593.467	0.029	24517.1	1.36
7998.502	10826.610	0.029	28054.8	1.55
9459.522	11059.603	0.029	34392.6	1.94
13843.045	11014.343	0.029	55504.3	3.11
16789.189	12295.258	0.029	70986.6	3.91
22103.247	10022.034	0.029	100627.1	5.46
24745.908	104444.898	0.029	116438.4	6.22

TABLE X

RAW DATA FOR TUBE NO: 4, RUN 10

<u>% FLOW</u>	<u>T_{ci} (°C)</u>	<u>T_{co} (°C)</u>	<u>T_v (°C)</u>	<u>GPM</u>
10	24.500	35.200	73.375	1.92
12.5	24.800	34.067	73.375	2.40
15	25.300	33.867	73.375	2.88
17.5	26.100	33.833	73.375	3.36
20	26.600	33.700	73.375	3.84
25	26.000	33.100	73.375	4.80
40	27.200	31.900	73.375	7.68
50	28.300	32.367	73.375	9.67
70	29.700	32.833	73.375	13.48
80	30.600	33.533	73.375	15.36

TABLE XI

RESULTS FOR TUBE NO: 4, RUN 10

$\underline{U_n}$	$\underline{U_c}$	\underline{Q}	$\underline{\dot{m}_c}$
2754.738	3270.101	5439.790	.002315
2950.654	3549.902	5890.343	.002507
3282.571	4041.559	6533.981	.002781
3484.748	4352.466	6879.525	.002928
3670.281	4645.789	7218.049	.003072
4526.156	6107.690	9025.343	.003842
4787.990	6594.309	9559.236	.004069
5308.371	7623.594	10410.942	.004432
5822.347	8730.418	11174.606	.004757
6328.286	9919.585	11915.378	.005072

$\underline{h_i}$	$\underline{h_o}$	\underline{C}	\underline{Re}	$\underline{C_{wv}}$
4565.227	16897.966	0.029	13869.1	.78
5432.063	13435.250	0.029	17190.5	.97
6295.645	14578.640	0.029	20691.5	1.17
7152.500	13823.001	0.029	24328.1	1.36
7975.173	13499.872	0.029	27906.8	1.55
9470.136	22301.564	0.029	34462.5	1.94
13792.792	14282.183	0.029	55140.0	3.11
16730.289	15655.474	0.029	70536.2	3.91
22049.547	15752.896	0.029	100184.6	5.46
24692.997	18110.924	0.029	115987.6	6.22

TABLE XII

RAW DATA FOR TUBE NO: 5, RUN 10

<u>% FLOW</u>	<u>T_{ci} (°C)</u>	<u>T_{co} (°C)</u>	<u>T_v (°C)</u>	<u>GPM</u>
10	24.900	36.067	73.375	1.92
12.5	25.150	34.733	73.375	2.40
15	25.750	34.500	73.375	2.88
17.5	26.450	34.567	73.375	3.36
20	27.050	34.267	73.375	3.84
25	26.400	32.867	73.375	4.80
40	27.650	32.433	73.375	7.68
50	28.700	32.767	73.375	9.67
70	30.050	33.167	73.375	13.48
80	31.000	33.767	73.375	15.36

TABLE XIII

RESULTS FOR TUBE NO: 5, RUN 10

U_n	U_c	Q	\dot{m}_c
2918.294	3503.168	5675.364	.002416
3087.244	3749.482	6089.610	.002592
3394.481	4212.551	6671.698	.002840
3704.291	4700.415	7219.136	.003073
3774.685	4814.341	7335.082	.003122
4129.802	5405.668	8220.336	.003499
4926.346	6860.610	9725.592	.004140
5357.143	7724.593	10408.808	.004431
5839.040	8768.006	11115.595	.004731
6015.076	9171.035	11239.183	.004784

h_i	h_o	C	Re	C_{wv}
4597.556	24649.985	0.029	14047.5	.78
5463.038	16498.431	0.029	17368.4	.97
6333.856	16770.374	0.029	20919.5	1.17
7195.785	17767.523	0.029	24595.4	1.36
8020.371	14851.253	0.029	28193.9	1.55
9478.999	15102.528	0.029	34520.9	1.94
13868.798	15485.062	0.029	55691.5	3.11
16804.731	16010.637	0.029	71105.7	3.91
22132.653	15827.522	0.029	100869.8	5.46
24778.577	15723.011	0.029	116717.2	6.22

TABLE XIV

CALCULATED U_n AND h_n VALUES FOR RUN 10 AND 11 BY USING ACTUAL
VAPOR TEMPERATURE

Run No: 10 Saturated		Run No: 11 Superheat	
U_n	h_n	U_n	h_n
4328.7910	15786.4551	3415.5756	7720.4862
3774.5253	10963.0027	2988.8119	5985.2128
3715.2327	10574.6464	2938.9285	5819.6943
4143.9365	13969.3079	3351.3064	7418.9868
4163.9537	14537.9795	3290.4901	7238.0133

TABLE XV

OUTSIDE HEAT TRANSFER COEFFICIENTS FOR RUN 1, 2 AND 3

Run No: 1 $h_n (\text{W/m}^2\text{-}^\circ\text{C})$	Run No: 2 $h_n (\text{W/m}^2\text{-}^\circ\text{C})$	Run No: 3 $h_n (\text{W/m}^2\text{-}^\circ\text{C})$
20410.6000	22051.0505	17982.7509
9211.6182	10891.4140	10026.5844
10419.5087	11583.6072	10907.6969
20683.4820	19188.1990	4420.6795
18039.4950	16858.8026	14247.8599

TABLE XVI

OUTSIDE HEAD TRANSFER COEFFICIENTS FOR RUN 4, 5 AND 6

Run No: 4 $h_n (\text{W/m}^2\text{-}^\circ\text{C})$	Run No: 5 $h_n (\text{W/m}^2\text{-}^\circ\text{C})$	Run No: 6 $h_n (\text{W/m}^2\text{-}^\circ\text{C})$
23968.0185	23357.4232	21608.6195
12797.6682	11543.5844	11008.3957
13595.7268	12902.0927	10491.5847
18680.0589	18936.9402	9614.5084
19960.6512	19348.2619	5027.7868

TABLE XVII

OUTSIDE HEAT TRANSFER COEFFICIENTS FOR RUN 7, 8 AND 9

Run No: 7 $h_n (W/m^2-^{\circ}C)$	Run No: 8 $h_n (W/m^2-^{\circ}C)$	Run No: 9 $h_n (W/m^2-^{\circ}C)$
28538.3804	26265.9234	21990.0288
18356.1272	14002.0691	13282.0589
15115.2214	12683.1094	12600.4265
12932.0973	11423.2917	16127.8443
12006.7075	10005.0352	18357.4732

TABLE XVIII

OUTSIDE HEAT TRANSFER COEFFICIENTS FOR RUN 10, 11 AND 12

Run No: 10 $h_n (W/m^2-^{\circ}C)$	Run No: 11 $h_n (W/m^2-^{\circ}C)$	Run No: 12 $h_n (W/m^2-^{\circ}C)$
13534.0540	16052.7204	13965.0102
12301.2512	11114.5881	10540.0521
11357.6936	10384.2246	10139.7836
15833.7770	14821.7962	13651.0698
16268.6326	15112.0203	13300.1873

TABLE XIX

DATA RESULTS FOR RUN 1, 2 AND 3

Run No: 1 \bar{h}_n/h_1	Run No: 2 \bar{h}_n/h_1	Run No: 3 \bar{h}_n/h_1
1.00000	1.00000	1.00000
0.72566	0.74696	0.77878
0.65394	0.67308	0.72138
0.74379	0.72235	0.60249
0.77179	0.73079	0.64045

TABLE XX

DATA RESULTS FOR RUN 4, 5 AND 6

Run No: 4 \bar{h}_n/h_1	Run No: 5 \bar{h}_n/h_1	Run No: 6 \bar{h}_n/h_1
1.00000	1.00000	1.00000
0.76697	0.74711	0.75472
0.70040	0.68220	0.66499
0.72014	0.71433	0.60998
0.74267	0.73714	0.53452

TABLE XXI

DATA RESULTS FOR RUN 7, 8 AND 9

Run No: 7 \bar{h}_n/h_1	Run No: 8 \bar{h}_n/h_1	Run No: 9 \bar{h}_n/h_1
1.00000	1.00000	1.00000
0.82104	0.76654	0.80200
0.72360	0.67199	0.72567
0.65579	0.61272	0.72761
0.60863	0.56636	0.74905

TABLE XXII

DATA RESULTS FOR RUN 10, 11 AND 12

Run No: 10 \bar{h}_n/h_1	Run No: 11 \bar{h}_n/h_1	Run No: 12 \bar{h}_n/h_1
1.00000	1.00000	1.00000
0.83186	0.84619	0.87737
0.76783	0.79014	0.82694
0.73945	0.82343	0.86459
0.81359	0.84703	0.88931

FIGURES

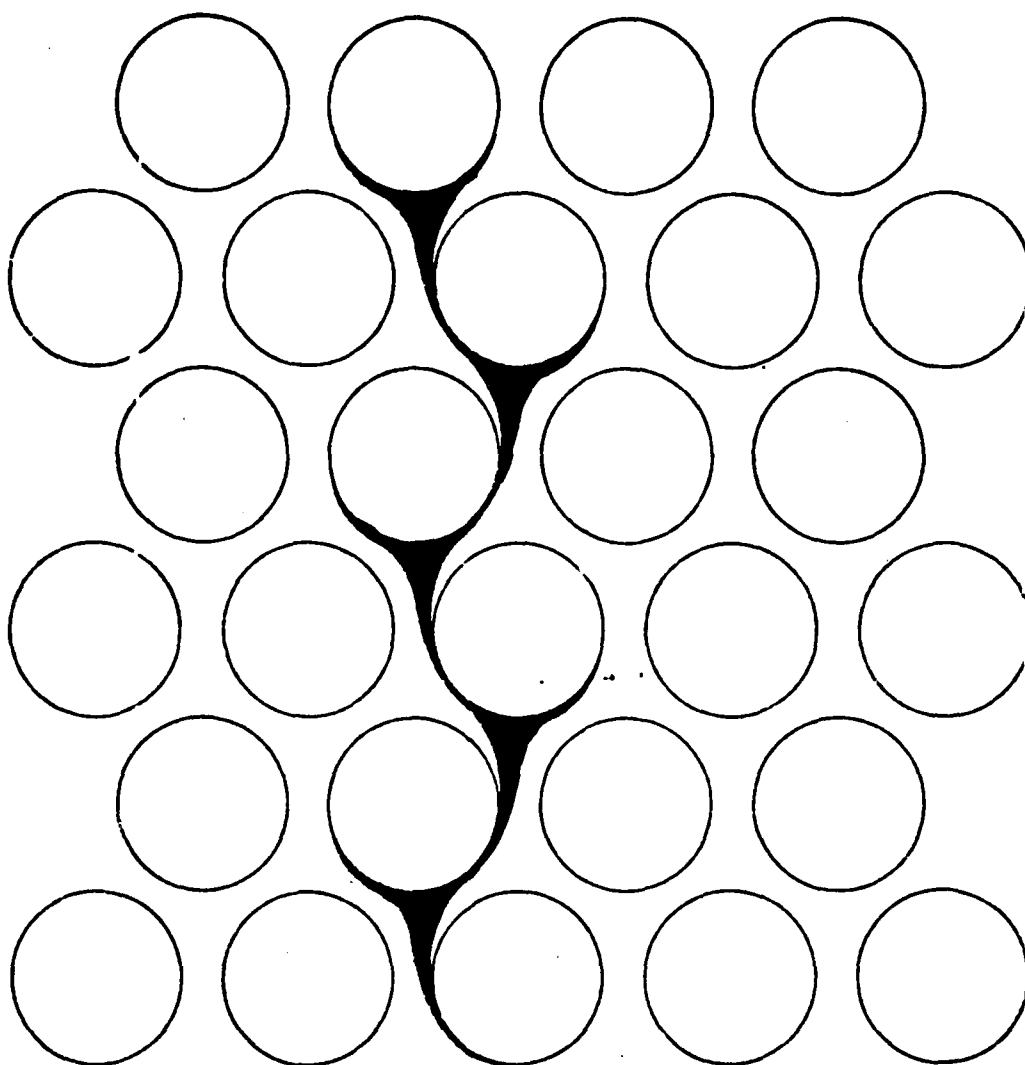


Fig. 1. Droplet Path Through a Tube Bundle with Side Drainage

STEAM SYSTEM

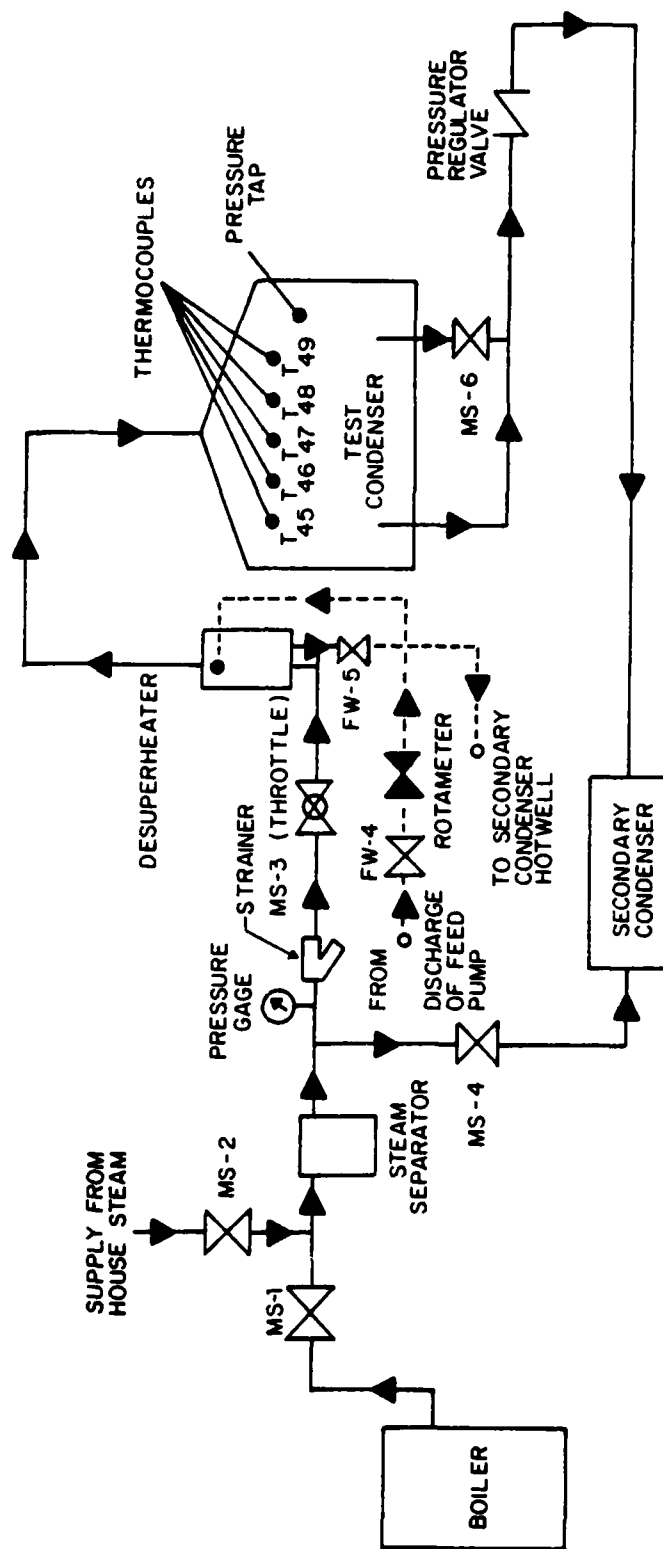


Fig. 2 Schematic Diagram of Steam System.

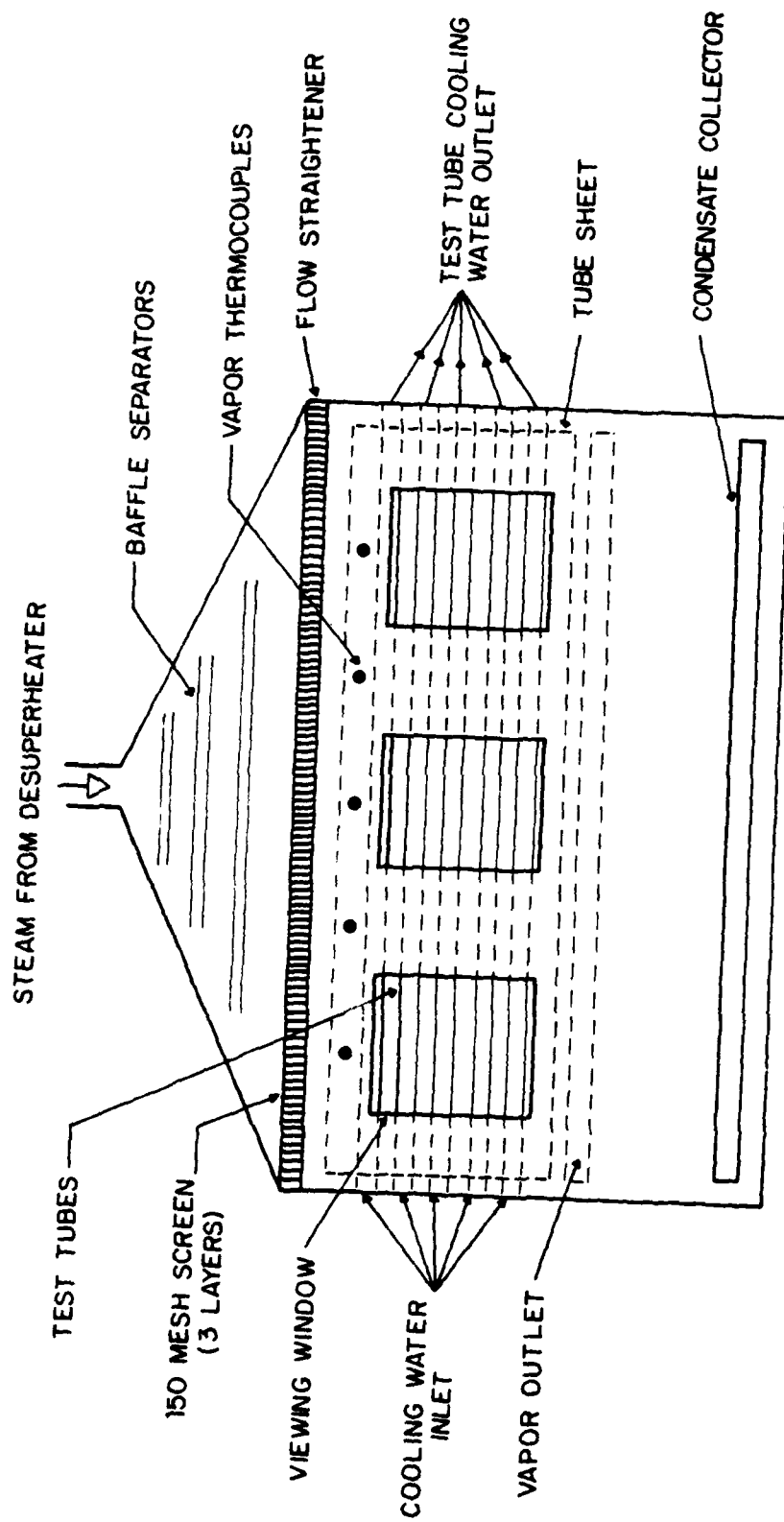


Fig. 3 Test Condenser Schematic, Front View.

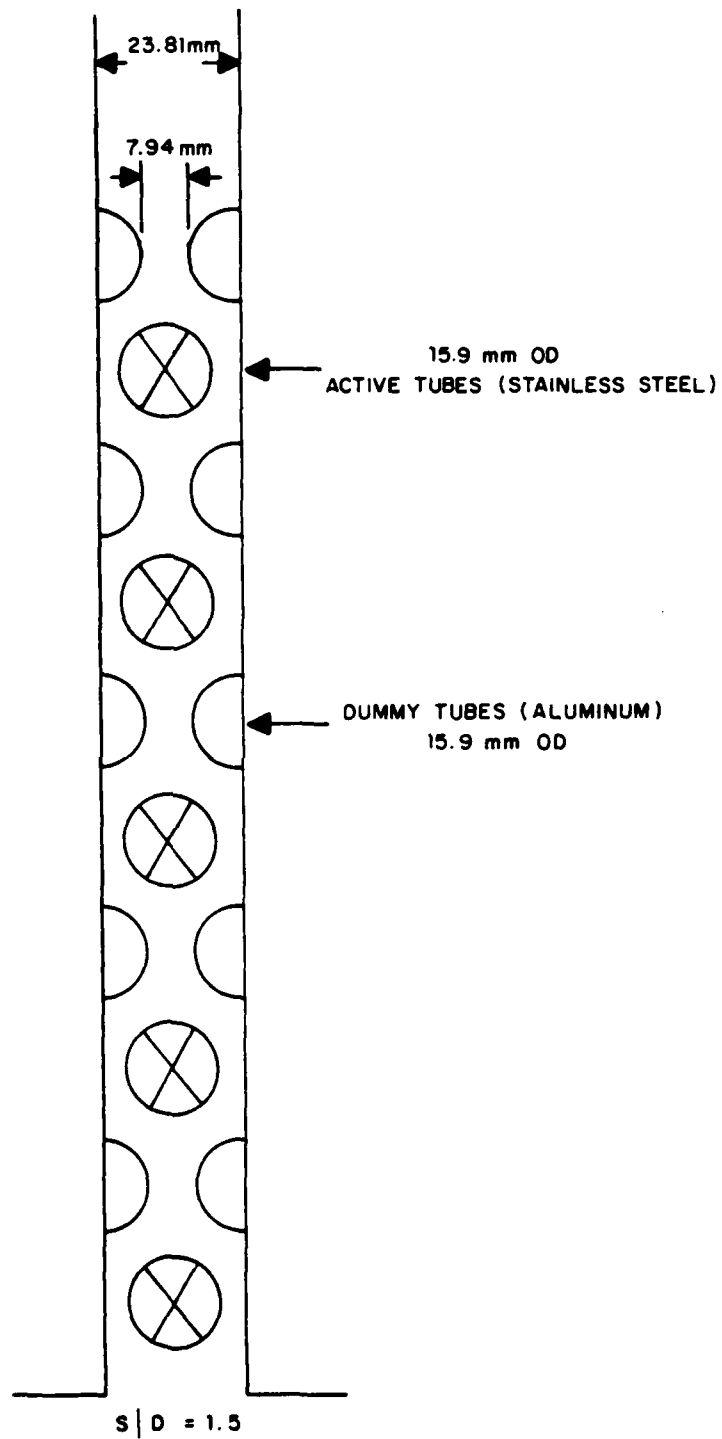


Fig. 4 Schematic Side View of Test Tube Arrangement.

CONDENSATE AND FEEDWATER SYSTEMS

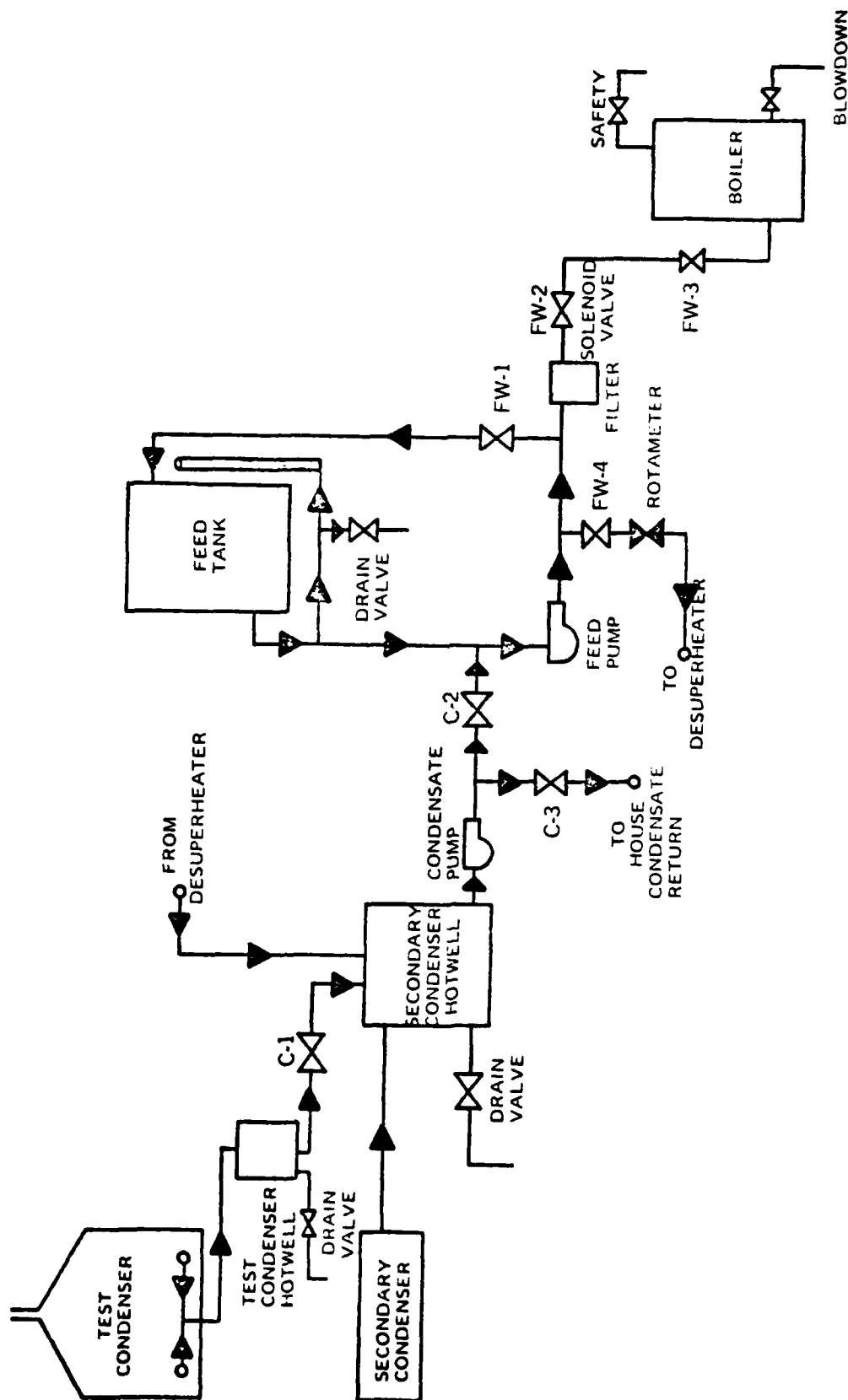


Fig. 5 Schematic Diagram of Condensate and Feedwater System

Fig. 6 Schematic Diagram of Cooling Water System.

VACUUM SYSTEM

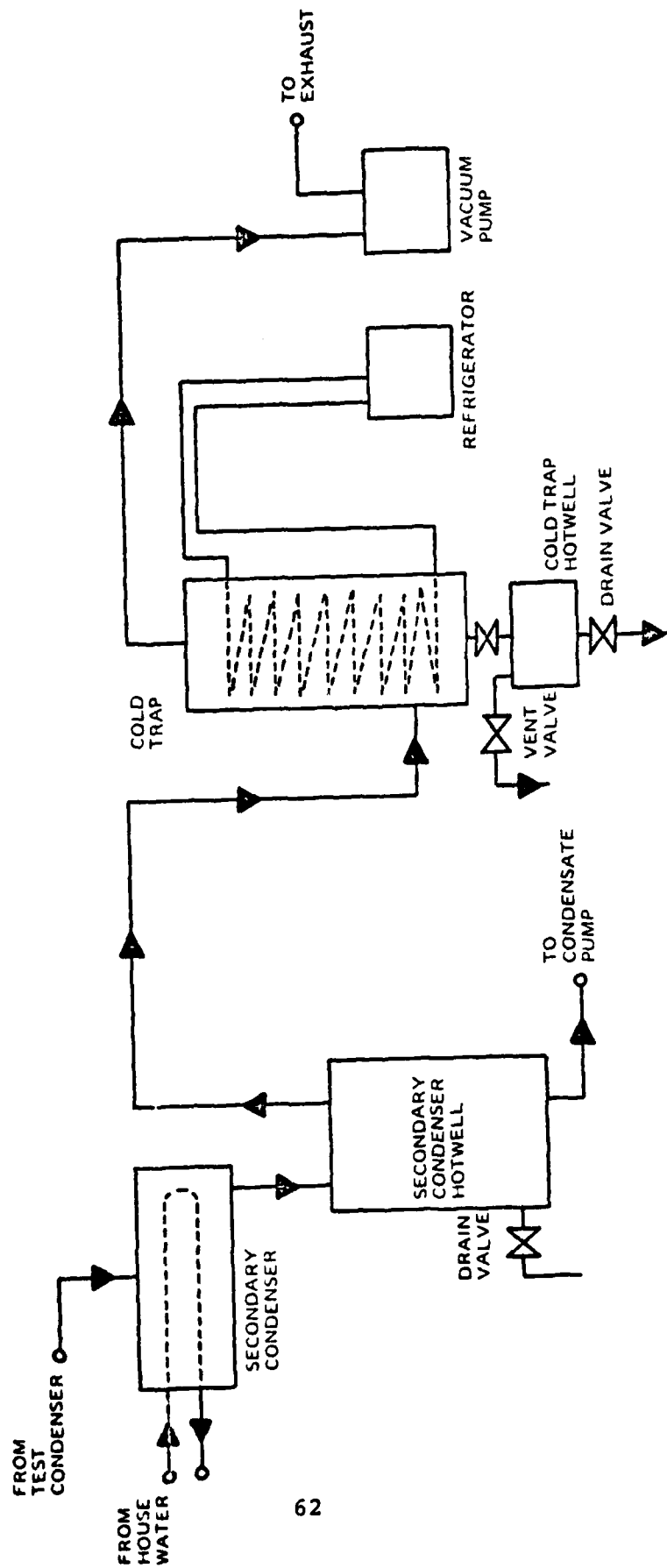


Fig. 7 Schematic Diagram of Vacuum System

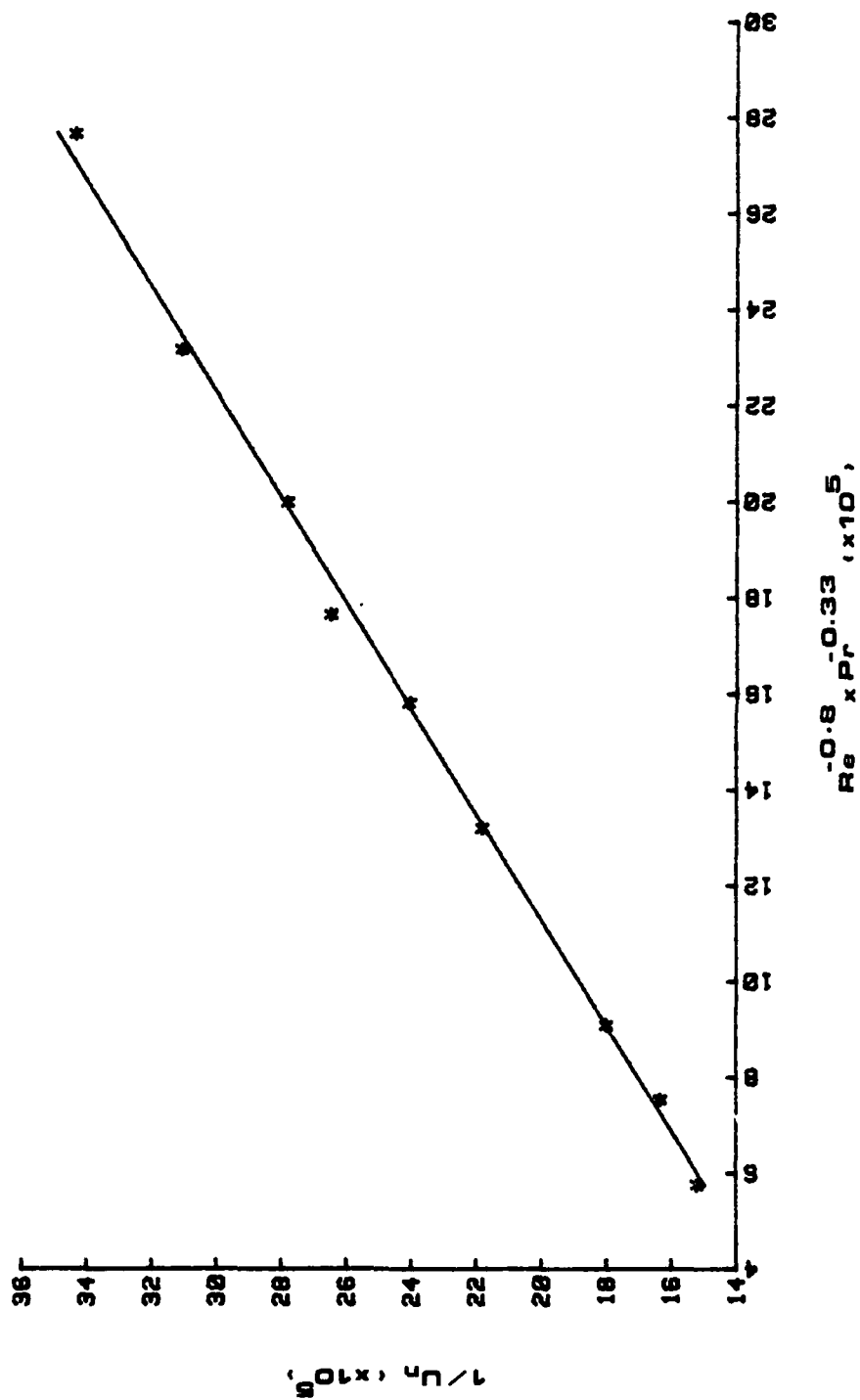


Fig. 8. Wilson Plot for Tube No:1, Run 10

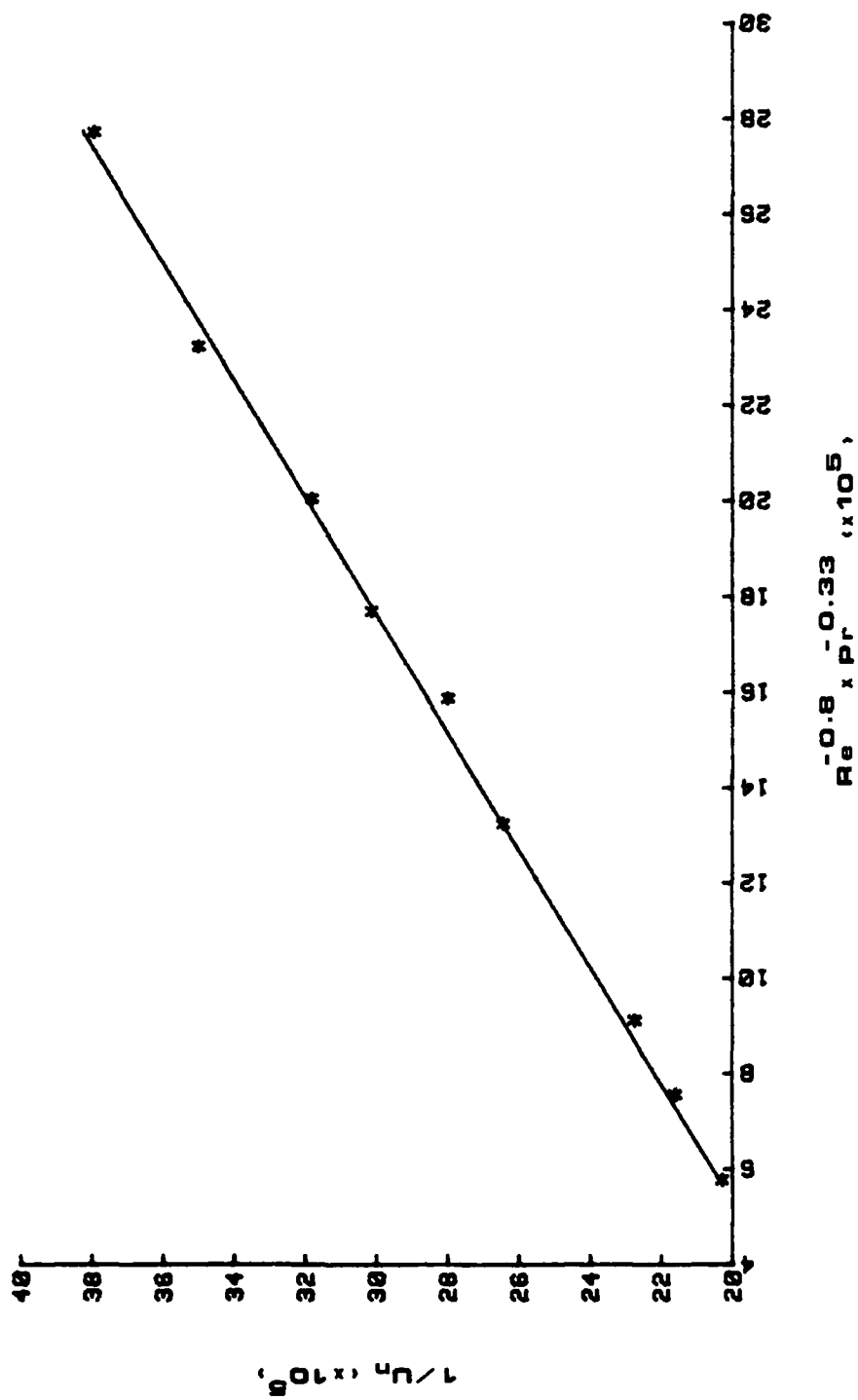


Fig. 9. Wilson Plot for Tube No:2, Run 10

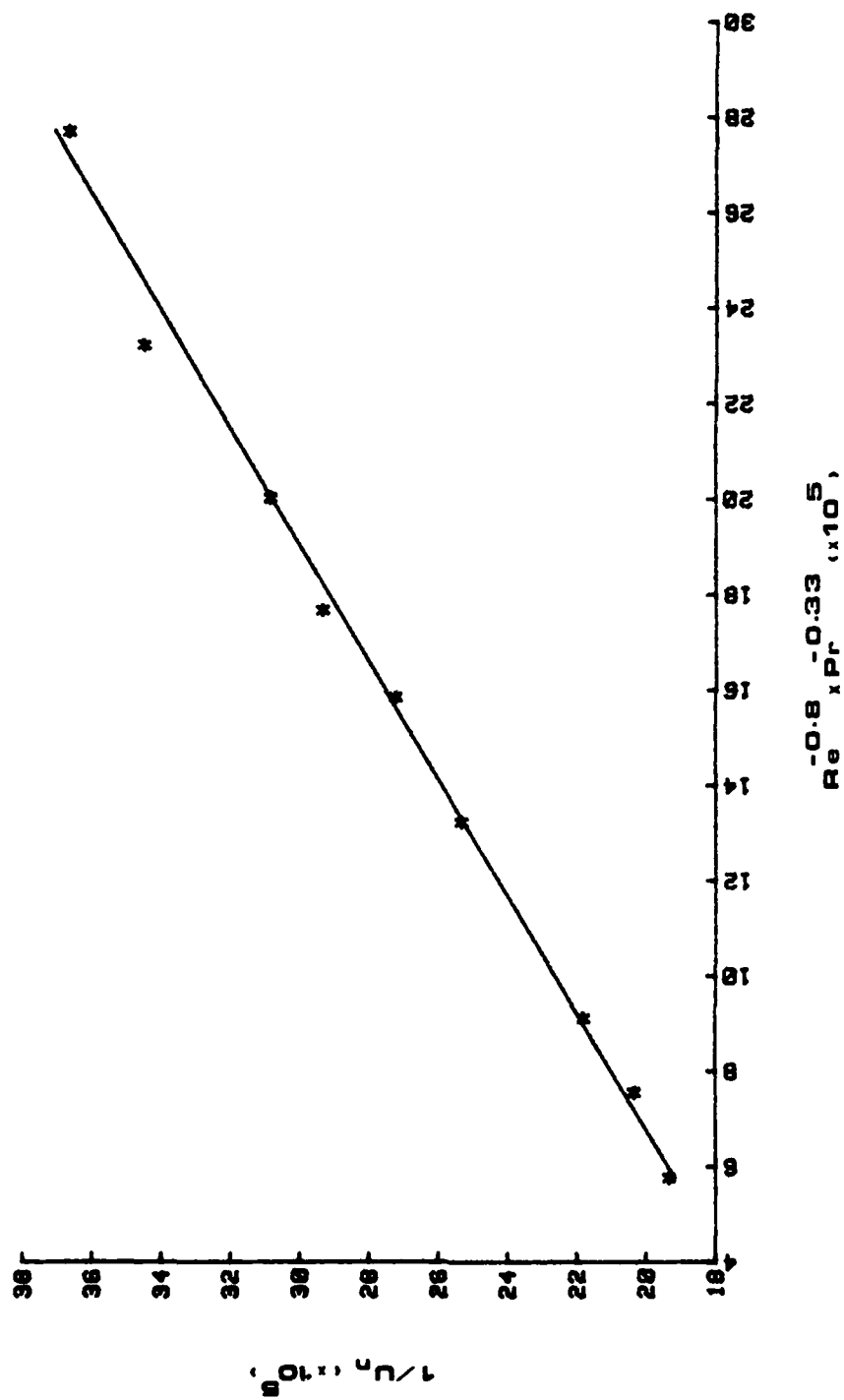


Fig. 10. Wilson Plot for Tube No:3, Run 10

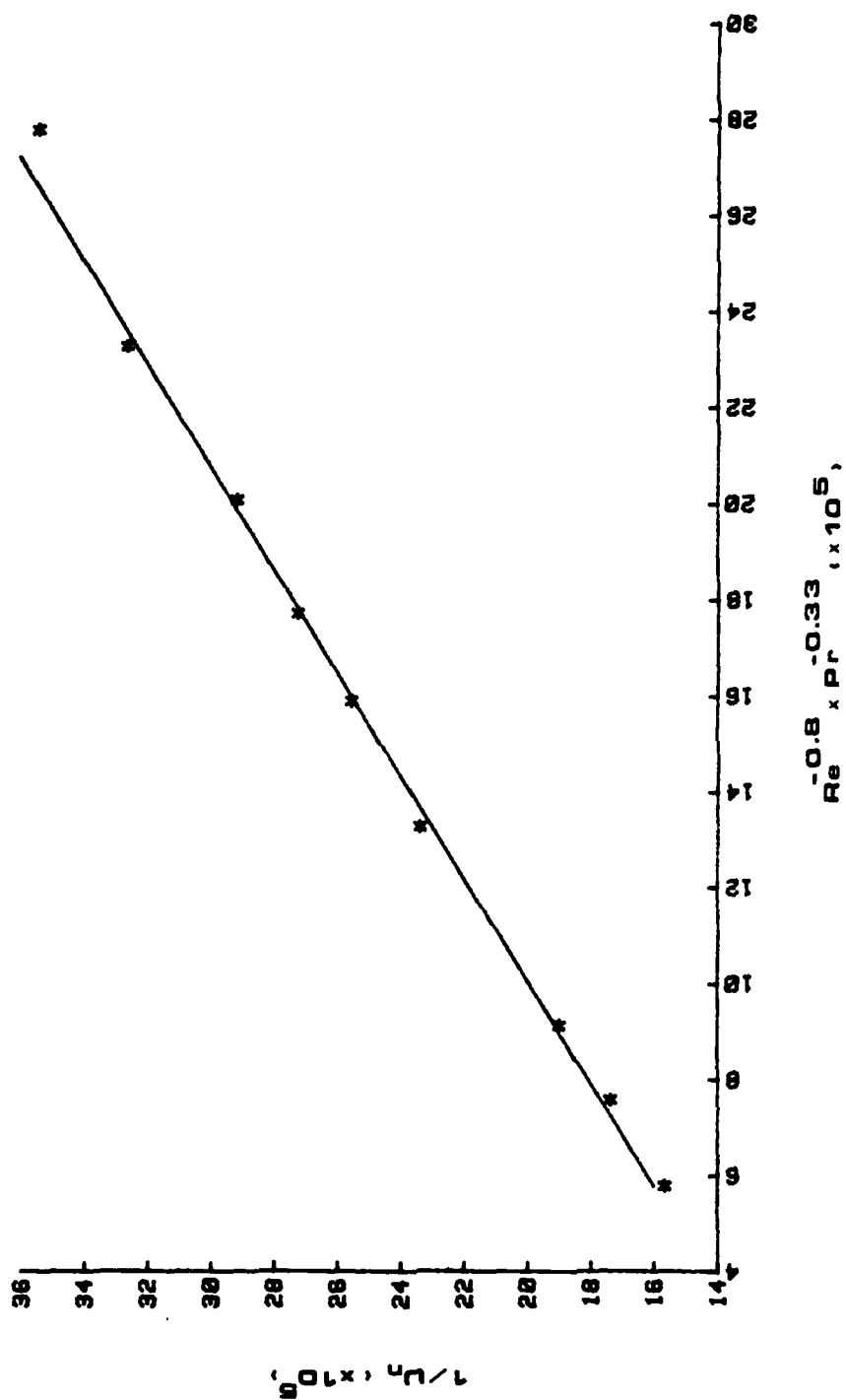


Fig. 11. Wilson Plot for Tube No:4, Run 10

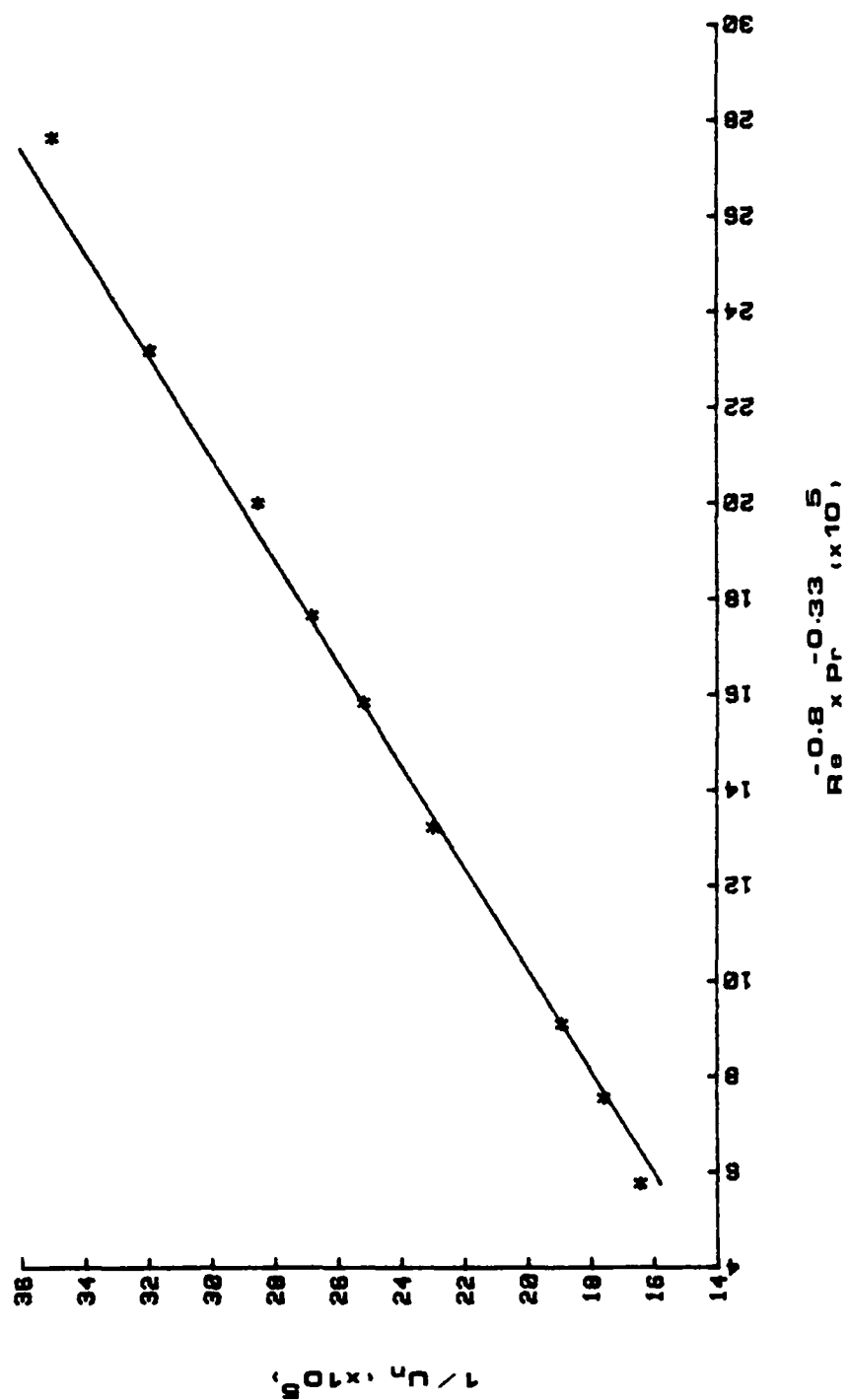


Fig. 12. Wilson Plot for Tube No:5, Run 10

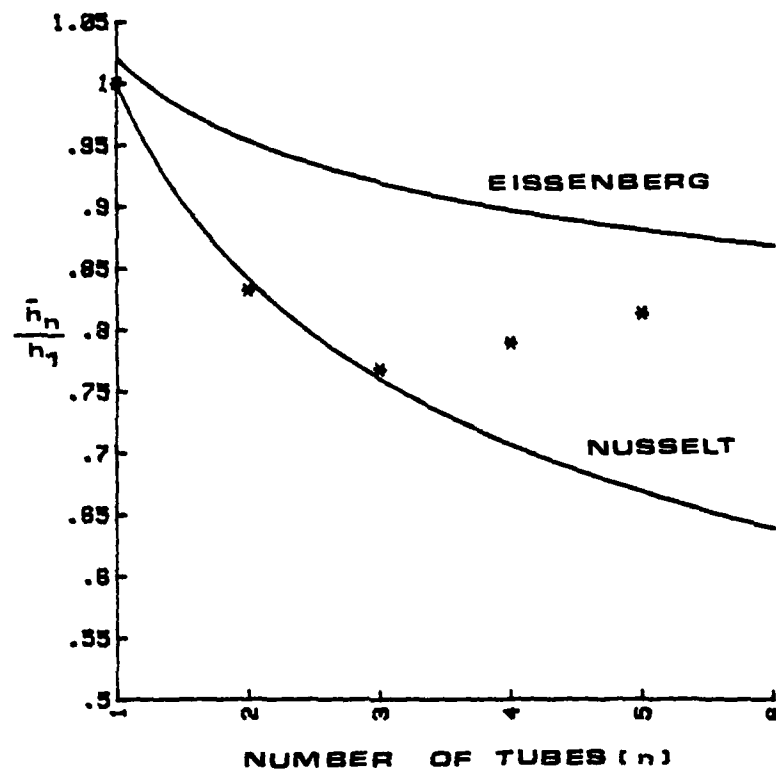


Fig. 13. Average Outside Heat Transfer Coefficient Ratio Versus Number of Tubes for Run No:10

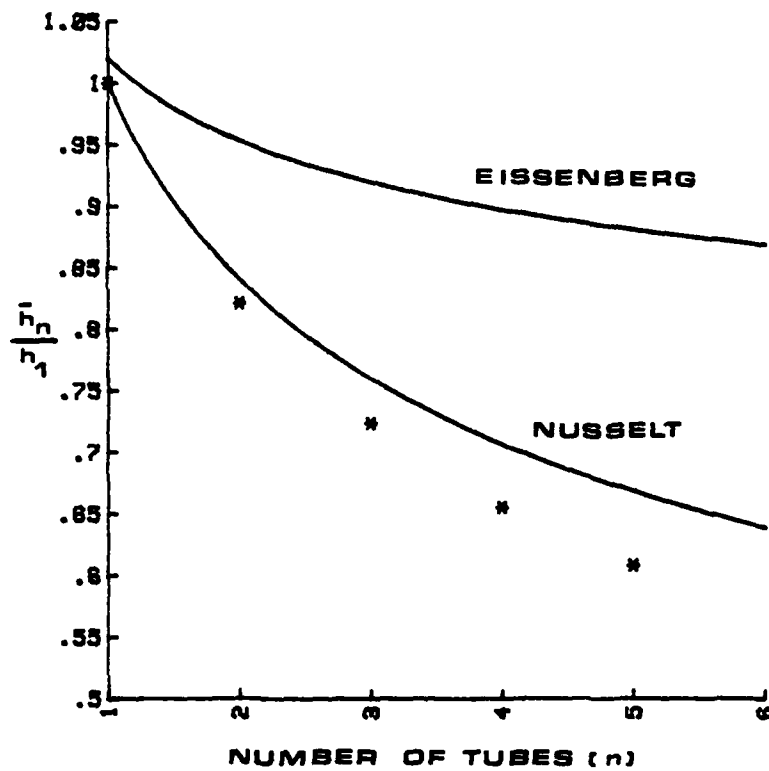


Fig. 14. Average Outside Heat Transfer Coefficient Ratio Versus Number of Tubes for Run No:7

APPENDIX A
TUBE CLEANING PROCEDURE

To ensure filmwise condensation, the condenser tubes had to be prepared. Surfaces of the tubes were cleaned to insure proper wetting characteristics and to insure that all deposits were removed. Stainless steel tubes were prepared in accordance with the procedure given in Newton [17]. The steps in this cleaning procedure are as follows:

1. Prepare an Alconox detergent solution and heat to 90 °C.
2. Apply this solution to the surface of the tubes.
3. Drain and rinse the tubes with distilled water.
4. Spray with alcohol.
5. Rinse with distilled water.
6. Spray with acetone
7. Rinse with distilled water.

APPENDIX B

SAMPLE CALCULATIONS

The following is an example of how the data reduction program calculates the results. Tube number one at 40 percent flow rate of cooling water of run 10 was selected for this analysis. This same tube and flow rate was used for the error analysis in Appendix C.

Input parameters

Tube Outside Diameter (D_o)	0.015875 m.
Tube Inside Diameter (D_i)	0.0141 m.
Tube Length (L_{ts})	0.9144 m.
Outside Nominal Surface Area (A_n)	0.0456 m ²
Wall Resistance (R_w)	5.72×10^{-5} m ² -K/W
Cooling Water Inlet Temperature (T_{ci})	27.7 °C
Cooling Water Outlet Temperature (T_{co})	32.7 °C
Average Cooling Water Temperature (T_{bc}, T_{bk})	30.2 °C, 303.4 K
Steam saturation temperature (T_v)	73.375 °C
Gallons Per Minute of Cooling Water (GPM)	7.68 GPM

Section 1. Water Properties

$$\mu \text{ (MHUW)} = (4.134 \times 10^{-4}) \text{ Exp } \left\{ \left[(0.00829158) (303.4) + (2644.2184) / (303.4) \right] - 10.59252566 \right\}$$

$$\mu = 7.828 \times 10^{-4} \text{ kg/m-sec}$$

$$k(KW) = 0.5565919 + (0.002174417)(30.2) - (0.70127 \times 10^{-5})(30.2)^2 \\ - (2.0914 \times 10^{-10})(30.2)^3$$

$$K = 0.615858 \text{ W/m}^{-\circ}\text{C}$$

$$\rho(RHO) = 1004.44434 - (0.12673368)(30.2) \\ - (0.0023913147)(30.2)^2$$

$$\rho = 998.436 \text{ kg/m}^3$$

$$C_p(CP) = 4.2377955 - (0.0018553514)(30.2) \\ + (1.3948314 \times 10^{-5})(30.2)^2$$

$$C_p = 4.195 \text{ kJ/kg}^{-\circ}\text{C}$$

$$\dot{m}(\text{MFRCW}) = \text{LPM} \times \text{RHO} \times 1.67 \times 10^{-5}$$

$$\text{where LPM} = \text{GPM} \times 3.78533$$

$$\dot{m} = (29.0713344)(998.436)(1.67 \times 10^{-5})$$

$$\dot{m} = 0.484732 \text{ kg/sec.}$$

$$\text{Prandtl Number (Pr)}$$

$$\text{Pr} = \mu C_p / k = (7.828 \times 10^{-4} \times 4.1945 \times 10^3) / (0.615858)$$

$$\text{Pr} = 5.3315$$

Section 2. Data Reduction

$$1. \text{ Cooling water velocity } (C_{CW}) = 4 \dot{m} / \rho \pi D_i^2$$

$$C_{CW} = (4 \times 0.484732) / [(998.436) \pi (0.0141)^2]$$

$$C_{CW} = 3.1092 \text{ m/sec}$$

2. Mass flow rate per unit area (G)

$$G = 4 \dot{m} / \pi D_i^2 = \rho C_{cw}$$

$$G = (998.436) (3.1092)$$

$$G = 3104.3372 \text{ kg/m}^2\text{-sec}$$

3. Reynolds Number (Re)

$$Re = D_i G / \mu = (0.0141 \times 3104.3372) / (7.828 \times 10^{-4})$$

$$Re = 55916.14$$

4. Overall Heat transfer Coefficient (U_n)

$$U_n = \frac{\dot{m} C_p}{A_n} \ln \left(\frac{T_v - T_{ci}}{T_v - T_{co}} \right)$$

$$= \frac{(0.484732) (4.1945 \times 10^3)}{0.0456} \ln \left(\frac{73.375 - 27.7}{73.375 - 32.7} \right)$$

$$= 5169.408 \text{ W / m}^2\text{-}^\circ\text{C}$$

5. Corrected Overall Heat Transfer Coefficient (U_c)

$$U_c = \frac{1}{\frac{1}{U_n} - R_w} = \frac{1}{\frac{1}{5169.408} - 5.72 \times 10^{-5}}$$

$$U_c = 7339.68 \text{ W / m}^2\text{-}^\circ\text{C}$$

6. Wilson Plot Parameters (X,Y)

(a) Ordinate

$$Y = \frac{1}{U_n} = \frac{1}{5169.408}$$

$$Y = 19.345 \times 10^{-5} \text{ m}^2\text{-}^\circ\text{C / W}$$

(b) Abscissa

$$X = \frac{1}{Re^{0.8} Pr^{1/3}} = \frac{1}{(55916.14)^{0.8} (5.3315)^{1/3}}$$

$$X = 9.114 \times 10^{-5}$$

7. Determination of constant

$$C = \frac{D_o}{Mk}$$

Where M = Slope returned by linear regression subroutine

$$M = 0.9265$$

$$C = \frac{0.015875}{(0.9265)(0.615858)}$$

$$C = 0.028$$

8. Inside Heat Transfer Coefficient (h_i)

$$Nu = \frac{h_i D_i}{k} = 0.036 Re^{0.8} Pr^{1/3} (L/D_o)^{-0.054}$$

where

$$\frac{L}{D} = \frac{0.9144}{0.015875} = 57.6$$

$$h_i = \frac{k}{D_i} (0.029) Re^{0.8} Pr^{1/3}$$

$$h_i = \frac{0.615858}{0.0141} (0.029) (55916.14)^{0.8} (5.3315)^{1/3}$$

$$h_i = 13898.64 \text{ W/m}^2\text{-}^\circ\text{C}$$

9. Outside Heat Transfer Coefficient (h_o)

$$h_o = \frac{1}{\frac{1}{U_n} - R_w - \frac{D_o}{D_i h_i}}$$

$$h_o = \frac{1}{\frac{1}{5169.408} - 5.72 \times 10^{-5} - \frac{0.015875}{(0.0141)(13898.64)}}$$

$$h_o = 18103.22 \text{ W/m}^2\text{-}^\circ\text{C}$$

APPENDIX C
ERROR ANALYSIS

The basic equations used in this section are reproduced from Reilly [15]. The general form of the Kline and McClintock [18] "second order" equation is used to compute the probable error in the results. For some resultant, R , which is a function of primary variables x_1, x_2, \dots, x_n , the probable error in R , δR is given by:

$$\delta R = \left[\left(\frac{\delta R}{\delta x_1} \delta x_1 \right)^2 + \left(\frac{\delta R}{\delta x_2} \delta x_2 \right)^2 + \dots + \left(\frac{\delta R}{\delta x_n} \delta x_n \right)^2 \right]^{1/2}$$

where $\delta x_1, \delta x_2, \dots, \delta x_n$ is the probable error in each of the measured variables.

1. Uncertainty in overall heat transfer coefficient, U_n

$$\frac{\delta U_n}{U_n} = \left\{ \left(\frac{\delta A_n}{A_n} \right)^2 + \left(\frac{\delta C_p}{C_p} \right)^2 + \left(\frac{\delta \dot{m}}{\dot{m}} \right)^2 + \left[\frac{\delta T_v (T_{ci} - T_{co})}{(T_v - T_{ci})(T_v - T_{co}) \ln \frac{T_v - T_{ci}}{T_v - T_{co}}} \right]^2 + \left[\frac{\delta T_{ci}}{(T_v - T_{ci}) \ln \frac{T_v - T_{ci}}{T_v - T_{co}}} \right]^2 + \left[\frac{\delta T_{co}}{(T_v - T_{co}) \ln \frac{T_v - T_{ci}}{T_v - T_{co}}} \right]^2 \right\}^{1/2}$$

The following values are assigned to the variables

$$\delta A_n = \pm 0.0001 \text{ m}^2$$

$$\delta C_p = \pm 0.0042 \text{ KJ/kg-}^\circ\text{C}$$

$$\delta \dot{m} = \pm 0.01 \text{ kg/sec}$$

$$\delta T_v = \pm 0.5 \text{ }^\circ\text{C}$$

$$\delta T_{ci} = \pm 0.1 \text{ }^\circ\text{C}$$

$$\delta T_{co} = \pm 0.1 \text{ }^\circ\text{C}$$

For tube No:1 at 40 percent of 10. run:

$$\begin{aligned} \frac{\delta U_n}{U_n} = & \left\{ \left(\frac{0.0001}{0.0456} \right)^2 + \left(\frac{0.0042}{4.1945} \right)^2 + \left(\frac{0.01}{0.484732} \right)^2 \right. \\ & + \left[\frac{(0.5)(-5)}{(45.675)(40.675) \text{Ln}(1.1229)} \right]^2 \\ & \left. + \left[\frac{0.1}{(40.675) \text{Ln}(1.1229)} \right]^2 + \left[\frac{0.1}{(45.675) \text{Ln}(1.1229)} \right]^2 \right\}^{1/2} \end{aligned}$$

$$\frac{\delta U_n}{U_n} = 0.037$$

2. Uncertainty in inside heat transfer coefficient, h_i

The probable error in the inside heat transfer coefficient is given by:

$$\frac{\delta h_i}{h_i} = \left[\left(\frac{\delta k}{k} \right)^2 + \left(\frac{\delta D_i}{D_i} \right)^2 + \left(\frac{0.8 \delta Re}{Re} \right)^2 + \left(\frac{0.333 \delta Pr}{Pr} \right)^2 + \left(\frac{\delta C}{C} \right)^2 \right]^{\frac{1}{2}}$$

where

$$\delta k = \pm 0.001 \text{ W/m}^\circ\text{C}$$

$$\delta D_i = \pm 0.001 \text{ m}$$

$$\delta Pr = \pm 0.10$$

$$\delta C = \pm 0.001$$

$$\begin{aligned} \frac{\delta Re}{Re} &= \left[\left(\frac{\delta G}{G} \right)^2 + \left(\frac{\delta \mu}{\mu} \right)^2 + \left(\frac{\delta D_i}{D_i} \right)^2 \right]^{\frac{1}{2}} \\ &= \left[(0.01)^2 + \left(\frac{0.1}{7.828} \right)^2 + \left(\frac{0.001}{0.0141} \right)^2 \right]^{\frac{1}{2}} \end{aligned}$$

$$\frac{\delta Re}{Re} = 0.073$$

$$\begin{aligned} \frac{\delta h_i}{h_i} &= \left[\left(\frac{0.001}{0.615858} \right)^2 + \left(\frac{0.001}{0.0141} \right)^2 + (0.8 \times 0.073)^2 + \left(0.333 \frac{0.10}{5.3315} \right)^2 + \left(\frac{0.001}{0.029} \right)^2 \right]^{\frac{1}{2}} \\ &= 0.098 \end{aligned}$$

$$h_i, \text{ Tube No:1_40\%_10.Run} = 13899 \pm 1362 \text{ W/m}^2\text{-}^\circ\text{C}$$

3. Uncertainty in outside heat transfer coefficient, h_o

The probable error in the outside heat transfer coefficient is given by:

$$\frac{\delta h_o}{h_o} = \left\{ \left[\frac{\delta U_n}{U_n^2 \left(\frac{1}{U_n} - R_w - \frac{D_o}{D_i h_i} \right)} \right]^2 + \left[\frac{\delta R_w}{\frac{1}{U_n} - R_w - \frac{D_o}{D_i h_i}} \right]^2 + \left[\frac{\frac{D_o}{D_i h_i} \frac{\delta h_i}{h_i}}{\frac{1}{U_n} - R_w - \frac{D_o}{D_i h_i}} \right]^2 \right\}^{\frac{1}{2}}$$

where $\frac{\delta U_n}{U_n} = 0.037$

$$\delta R_w = 2.86 \times 10^{-6} \text{ m}^2\text{-}^\circ\text{C/W}$$

$$\frac{\delta h_i}{h_i} = 0.098$$

$$\frac{1}{U_n} - R_w - \frac{D_o}{D_i h_i} = 5.524 \times 10^{-5} \text{ m}^2\text{-}^\circ\text{C/W}$$

$$\frac{\delta h_o}{h_o} = \left\{ \left[\frac{0.037}{(5169.408)(5.524 \times 10^{-5})} \right]^2 + \left[\frac{2.86 \times 10^{-6}}{5.524 \times 10^{-5}} \right]^2 + \left[\frac{(8.10 \times 10^{-5})(0.098)}{(5.524 \times 10^{-5})} \right]^2 \right\}^{\frac{1}{2}}$$

$$\frac{\delta h_o}{h_o} = 0.200$$

$$h_o, \text{ Tube No:1-40\%-10.Run} = 18103 \pm 3621 \text{ W/m}^2\text{-}^\circ\text{C}$$

LIST OF REFERENCES

1. Standards for Steam Surface Condensers, 6th ed., Heat Exchange Institute, 1970.
2. Standards of Tubular Exchanger Manufacturers Association, 4th ed., Tubular Exchanger Manufacturers Association, Inc., 1959.
3. Search, H.T., A Feasibility Study of Heat Transfer Improvement in Marine Steam Condensers, MSME, Naval Postgraduate School, Monterey, California, December 1977.
4. Eshleman, D.E., An Experimental Investigation of the Effect of Condensate Inundation on Heat Transfer in a Horizontal Tube Bundle, MSME, Naval Postgraduate School, Monterey, California, March 1980.
5. Jakob, M., Heat Transfer, Vol. I, 8th edition, John Wiley & Sons Inc., May 1962.
6. Eissenberg, D.M., An Investigation of the Variables Affecting Steam Condensation on the Outside of a Horizontal Tube Bundle, Ph.D. Thesis, University of Tennessee, Knoxville, December 1972.
7. Fujii, T., "Vapor Shear and Condensate Inundation", Research Institute of Industrial Science, Kijushu University, Fukuoka, Japan, 1979.
8. Nobbs, D.W. and Mayhew, Y.R., "Effect of Downward Vapor Velocity and Inundation Rates on Horizontal Tube Banks", Steam Turbine Condensers, NEL Rept No. 619, pp. 39-52, 1976.
9. Nobbs, D.W., "The effect of Downward Vapor Velocity and Inundation on the Condensation Rates on Horizontal Tubes and Tube Banks", Ph.D. Thesis, Bristol University, April 1975.
10. Chisholm, D., "Proc. Workshop on Modern Developemnts in Marine Condensers", Naval Postgraduate School, Monterey, California, 26-28 March 1980.
11. Berman, L.D. and Tumanov, V.A., "Investigation of Heat Transfer during the Condensation of Flowing Steam on a Horizontal Tube Bundle", Teploenergetika, Vol. 9, No. 10, pp. 77-83, 1962.

12. Fuks, S.N., "Heat Transfer with condensation of Steam Flowing in a Horizontal Tube", Teploenergetika, Vol. 4, No. 1, pp. 35-38, 1957. English translation: NEL 1041, National Engineering Laboratory, East Kilbride, Glasgow.
13. Beck, A.C., A Test Facility to Measure Heat Transfer Performance of Advanced Condenser Tubes, MSME, Naval Postgraduate School, Monterey, California, January 1977.
14. Pence, D.T., An Experimental Study of Steam Condensation on a Single Horizontal Tube, MSME, Naval Postgraduate School, Monterey, California, March, 1978.
15. Reilly, D.J., An Experimental Investigation of Enhanced Heat Transfer on Horizontal Condenser Tubes, MSME, Naval Postgraduate School, Monterey, California, March 1978.
16. Ciftci, H., An Experimental Study of Filmwise Condensation on Horizontal Enhanced Condenser Tubing, MSME, Naval Postgraduate School, Monterey, California, December 1979.
17. Newton, W.H., Performance Characteristics of Rotating Non-Capillary Heat Pipes, MSME, Naval Postgraduate School, Monterey, California, 1971.
18. Kline, S.J. and McClintock, F.A., Describing Uncertainties in Single Sample Experiments, Mech. Engin., Vol. 74, pp. 3-8, January 1953.

INITIAL DISTRIBUTION LIST

	No. Copies
1. Defense Technical Information Center Cameron Station Alexandria, Virginia 22314	2
2. Library, Code 0142 Naval Postgraduate School Monterey, California 93940	2
3. Department Chairman, Code 69 Department of Mechanical Engineering Naval Postgraduate School Monterey, California 93940	2
4. Professor P.J. Marto, Code 69Mx Department of Mechanical Engineering Naval Postgraduate School Monterey, California 93940	5
5. Professor Robert H. Nunn, Code 69 Nn Department of Mechanical Engineering Naval Postgraduate School Monterey, California 93940	1
6. Deniz Kuvvetleri Komutanligi Egitim Daire Baskanligi Bakanliklar, Ankara/TURKEY	2
7. Deniz Harp Okulu Komutanligi Heybeliada, Istanbul/TURKEY	1
8. Dz. Yzb. Ismail Demirel Tabaklar Mahallesi Acar Sokak NO 12 Bolu/TURKEY	2
9. Istanbul Teknik Universitesi Makina Fakultesi Istanbul/TURKEY	1

**DAT
FILM**